UNIVERSITYᴼᶠ BIRMINGHAM

The osteology of the Late Triassic reptile Scleromochlus taylori from µCT data

Foffa, Davide; Nesbitt, Sterling J.; Butler, Richard J.; Brusatte, Stephen L.; Walsh, Stig; Fraser, Nicholas C.; Barrett, Paul M.

Document Version
Publisher's PDF, also known as Version of record

Link to publication on Research at Birmingham portal

AR The Anatomical Record WILEY

The osteology of the Late Triassic reptile *Scleromochlus taylori* from μCT data

Davide Foffa[1,2,3] | Sterling J. Nesbitt[2] | Richard J. Butler[3] |
Stephen L. Brusatte[1,4] | Stig Walsh[1,4] | Nicholas C. Fraser[1,4] |
Paul M. Barrett[5]

[1]Department of Natural Sciences, National Museums Scotland, Edinburgh, UK

[2]Department of Geosciences, Virginia Tech, Blacksburg, Virginia, USA

[3]School of Geography, Earth and Environmental Sciences, University of Birmingham, Birmingham, UK

[4]School of GeoSciences, University of Edinburgh, Grant Institute, Edinburgh, UK

[5]Fossil Reptiles, Amphibians and Birds Section, Natural History Museum, London, UK

Correspondence
Davide Foffa, Department of Natural Sciences, National Museums Scotland, Chambers Street, Edinburgh EH1 1JF, UK.
Email: davidefoffa@vt.edu

Abstract

Scleromochlus taylori is one of the most enigmatic members of the herpeto-fauna from the Lossiemouth Sandstone Formation (Upper Triassic) of Elgin (Moray, Scotland). For many years it was thought to be closely related to pterosaurs and dinosaurs, but the anatomy of this animal is difficult to interpret because of the notoriously poor preservation of the six available specimens, which comprise void space in the sandstone after the bones were destroyed by diagenesis. Historically, these fossils have been studied using physical molds, which provide only incomplete, and potentially distorted, information. Due to these uncertainties, interpretations of the anatomy, phylogenetic relationships, and paleobiology of *Scleromochlus taylori* have remained contentious. Here, we use microcomputed tomographic (μCT) techniques to redescribe and illustrate the osteology of *Scleromochlus* in detail, building upon a short redescription of keystone features of the anatomy that we recently published. We digitally visualize, describe, and figure previously inaccessible—and thus unaltered—portions of its skeleton, as well as providing new observations on the exposed parts of each specimen. This work reveals many novel features of the skull, mandible, trunk, tail, girdles, forelimb, and hindlimb (particularly of the manus, femur, and pes), demonstrating that historic molding techniques failed, in some cases, to accurately capture the anatomy of *Scleromochlus*. Our review sheds light on some of the most controversial aspects of *Scleromochlus* morphology showing that this taxon retains plesiomorphic features of Aveme-tatarsalia in the postcranial skeleton, alongside a suite of synapomorphies diagnostic of pterosauromorphs (the broad clade of pterosaurs and taxa more closely related to them than dinosaurs), particularly one subgroup, the lagerpe-tids. Consistent with recent work, our updated phylogenetic analyses (Maximum Parsimony and Bayesian Inference) demonstrate that *Scleromochlus taylori* is an avemetatarsalian archosaur that is recovered firmly in an

early diverging position within Pterosauromorpha, as a member of Lagerpetidae, thus shedding important information on the origin of pterosaurs, the first group of vertebrates to evolve powered flight.

KEYWORDS

Elgin Reptiles, Lagerpetidae, Pterosauromorpha

1 | INTRODUCTION

Scleromochlus taylori is one of the most iconic, historically important and enigmatic Triassic reptiles. Historically considered to be a form close to either pterosaur or dinosaur origins (Bennett, 1996, 2013, 2020; Benton, 1999; Gauthier, 1984, 1986; Gauthier et al., 1988; Padian, 1984; Sereno, 1991; Woodward, 1907), many aspects of its anatomy and phylogenetic relationships have been poorly understood. *Scleromochlus* is a small reptile of the Upper Triassic (∼Carnian) fauna of the Lossiemouth Sandstone Formation (LSF) from the North-West of Scotland (UK) (Benton & Walker, 1985). The LSF fauna is a diverse assemblage of Triassic tetrapods that includes a procolophonid parareptile (*Leptopleuron*), a lepidosauromorph (*Brachyrhynodon*), and a variety of archosauromorphs, comprising a rhynchosaur (*Hyperodapedon*), four pseudosuchians (*Stagonolepis, Erpetosuchus, Ornithosuchus, "Dasygnathoides"*), and two avemetatarsalians (*Saltopus, Scleromochlus*; Benton, 1983, 1999; Benton & Walker, 1985, 2002, 2011; Foffa et al., 2020, 2022; Fraser & Benton, 1989; Newton, 1894; Säilä, 2010; Von Baczko & Ezcurra, 2016; Walker, 1964).

Studying the "Elgin Reptiles" has been difficult because of their preservation as either fragile crumbled bones or voids in the sandstone (Benton & Walker, 1985). Most of the available information on these specimens comes from peels made of rubbery materials (PVC, silicone) that were made by infilling both natural voids and the cavities left after removing soft, "rotten" bones from the matrix (Bennett, 2020; Benton & Walker, 1985, 2002; Walker, 1964; Figures 1 and 2). However, it has been shown that this technique does not capture all the available anatomical details from these specimens, because the casting material is too viscous to reach smaller cavities (Foffa et al., 2020, 2022; Figures 1c,d and 2): moreover, it cannot be used to access elements that are still deeply embedded in the matrix. Furthermore, remaining bone material (or unremoved cast fragments) acts as a barrier for further casting cycles and can also create molding artifacts that can alter the perception of the preserved anatomy. Finally, this procedure is destructive: the original blocks need to be broken into pieces to expose as much of the skeletons as possible, the remaining bone material has to be mechanically or chemically removed before proceeding with the molding, and grains of sandstone are removed at each peeling cycle, altering the specimens permanently. For all of these reasons, the reliability of next-generation peels to capture the true
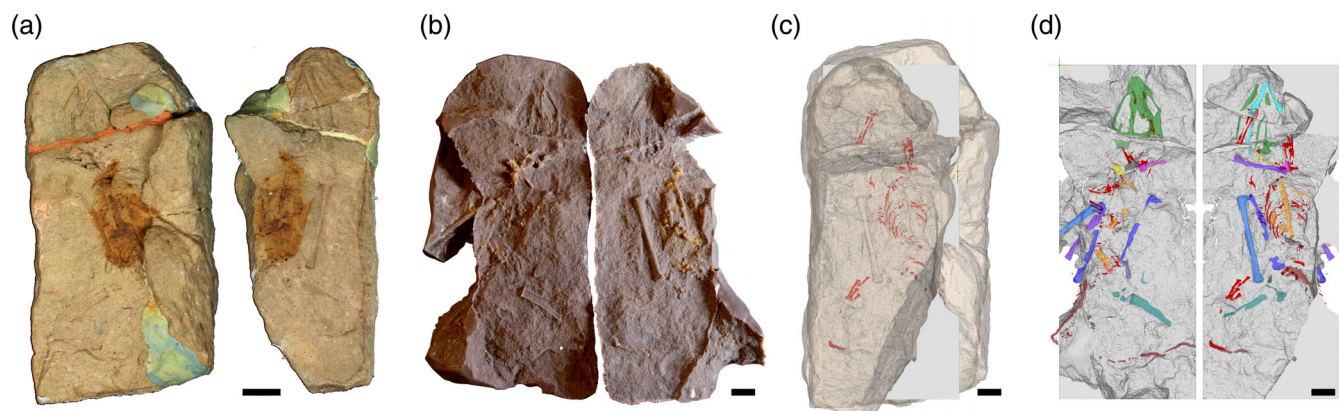
FIGURE 1 Diagram of the workflow methods applied to our study of *Scleromochlus taylori* (NHMUK PV R3557). (a) Original specimen showing the cavities left in multiple sandstone blocks (dorsal slab on the left, ventral slab on the right). (b) PVC cast of the cavities left in the sandstone. Note the need to take separate peels for the dorsal and ventral blocks. (c) Digital model of the specimen with new data highlighted in red (ventral view). (d) Digital rendering of the peel in dorsal (left) and ventral (right) views. Digital renderings of the peels are modelled in grey and novel data in red in c and d, and identifiable anatomical areas in the peel are highlighted in different colors in d (see Data S3 for more details of each specimen). Scale bars equal 10 mm.
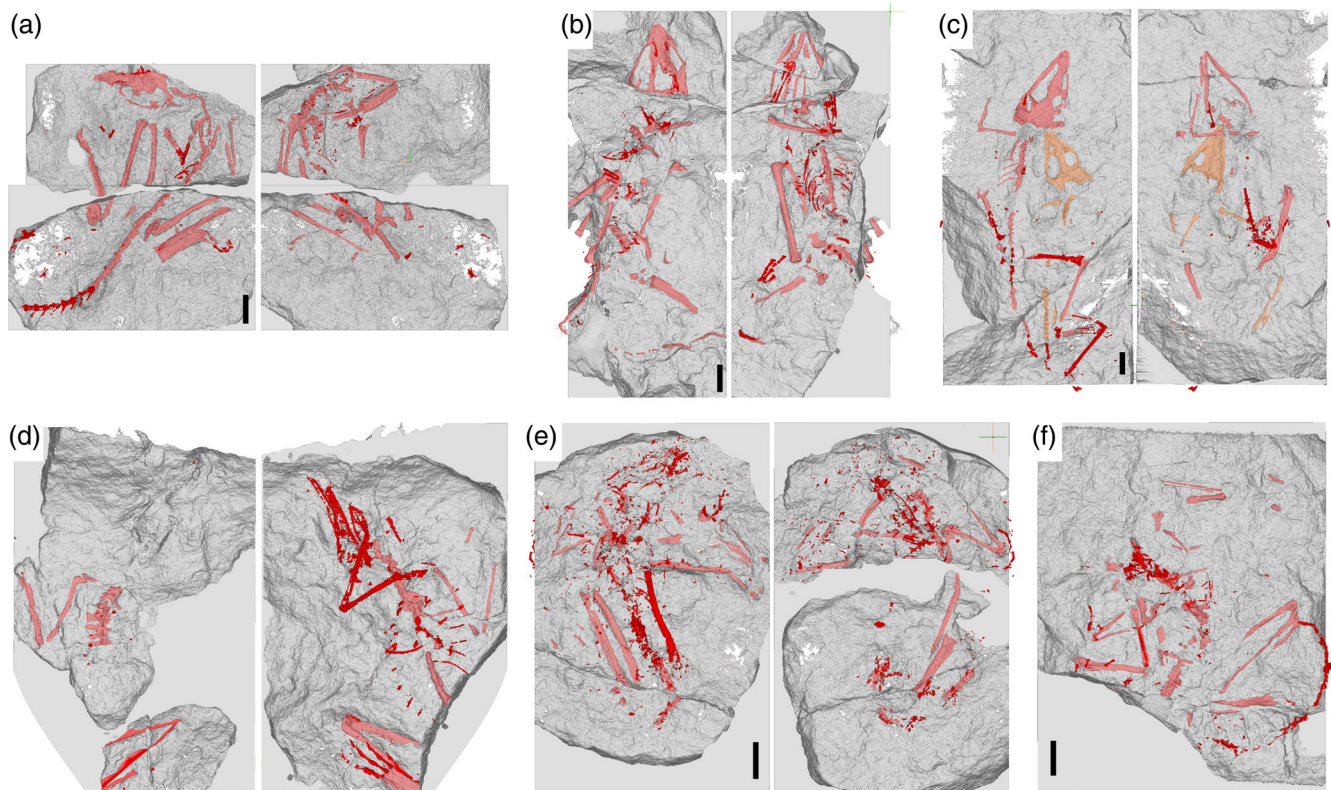
FIGURE 2 Digital reconstructions of all *Scleromochlus taylori* specimens. (a) Holotype, NHMUK PV R3556. (b) NHMUK PV R3557. (c) NHMUK PV R3146. (d) NHMUK PV R3914. (e) NHMUK PV R4823/4. (f) NHMUK PV R5589. Digital rendering of the peels in grey; previously unavailable details are figured in bright red; pink (and orange for individual b in NHMUK PV R3146) indicates skeletal elements identified in the peels. Dorsal and ventral views, respectively, on the left and right in a–e. Scale bars equal 10 mm.

morphology of these specimens has been questioned (Bennett, 2020). These issues are particularly marked with respect to the smaller members of the fauna, whose individual elements are close to the maximum resolution enabled by physical molding techniques. New discoveries of fossils from the LSF are extremely rare, meaning that virtually all interpretations are based on these historical specimens.

Scleromochlus is the smallest tetrapod from the LSF fauna (at most measuring ∼20 cm from snout to tip of the tail) and, consequently, traditional molding techniques are less effective than for other larger taxa. This, combined with some unusual aspects of the available skeletons, means that interpretations of the anatomy and phylogenetic position of this taxon have long been controversial (Foffa et al., 2022). Until recently, most studies—which largely rely on information from the detailed account by Benton (1999)—have recovered *Scleromochlus* as an ornithodiran archosaur closely related to pterosauromorphs (e.g., Benton, 1999; Ezcurra, Nesbitt, et al., 2020), but it has also been hypothesized to have affinities with basal archosauromorphs (Bennett, 2020), doswellids (Bennett, 2020), pseudosuchians (von Huene, 1908, 1913, 1914), and many different positions within Avemetatarsalia (Bennett, 1996,

2013; Gauthier, 1984, 1986; Kuhn, 1967; Nesbitt et al., 2017; Padian, 1984; Sereno, 1991; Young, 1964). Recently, the use of μCT allowed us to reevaluate the evolutionary relationships of *Scleromochlus*, and we recovered it as an early-branching pterosauromorph within Lagerpetidae (Foffa et al., 2022). Our study, however, presented only a brief overview of the most important, phylogenetically informative features of the skeleton. The markedly different interpretations that different authors have drawn from the available specimens have been at the core of these debates. Due to difficulties in interpreting its anatomy, many authors have excluded *Scleromochlus* from their analyses (or at least the primary versions of them; Ezcurra, 2016; Ezcurra, Jones, et al., 2020; Nesbitt, 2011; Nesbitt et al., 2017). This is unfortunate given the spatiotemporal occurrence of *Scleromochlus*, which—as a rare example of a Carnian-aged avemetatarsalian from the Northern Hemisphere—could have a potentially important impact on evolutionary and biogeographical scenarios.

To tackle this issue and build upon our short Foffa et al. (2022) article, we provide the first detailed and richly illustrated osteological description of *Scleromochlus* to be conducted using information derived from three-dimensional models built from microcomputed

TABLE 1   New information obtained from μCT scans for each specimen/individual of *Scleromochlus taylori*.

Specimen/individual	Voxel size (mm)	New elements revealed by μCT scans
NHMUK PV R3556	0.0670454	Skull fragments (maxilla, orbital area); hyoid; cervical ribs; dorsal ribs; middle and posterior caudal vertebrae; distal end of the humerus (L); proximal half of radius and ulna (L); pedal finger IV (R); pedal phalanges (L); unidentified fragments.
NHMUK PV R3557	0.0794120	Skull fragments (maxilla; postorbital area);? pectoral girdle; cervical and dorsal vertebrae; dorsal and caudal ribs; Radius, ulna, hand (L); incomplete foot (phalanges) (R); unidentified fragments.
NHMUK PV R3146A	0.0998629	Posterior right mandibular ramus; centra of dorsal vertebrae; middle caudal vertebrae; proximal femur (L); shaft and distal femur (R); distal tibia and fibula (R); metatarsals, and foot (R); unidentified fragments.
NHMUK PV R3146B	0.0998629	Caudal vertebrae; distal femur (R); tibia and fibula (R); fragments of metatarsal (R); unidentified fragments.
NHMUK PV R3914	0.0540913 and 0.040854	Skull elements; complete forelimb (R); shoulder girdle (?coracoids); dorsal vertebrae and ribs; fibula shaft (R); foot (phalanges and unguals) (R); unidentified fragments.
NHMUK PV R4823/4	0.057322	Skull or mandible fragments; cervical and dorsal vertebrae and ribs (fragments); caudal vertebrae; pelvic girdle fragments; nearly complete right femur; disarticulated and incomplete feet (L and R); unidentified fragments.
NHMUK PV R5589	0.0612608	Cervical/dorsal vertebrae and ribs (fragments); articulated series of middle and distal caudal vertebrae; pedal phalanges (L); unidentified fragments.

tomography (μCT) scans. We verified the new information against the original specimens and multiple generations of casts and peels to ensure their reliability. Using μCT has multiple advantages, and this technique has proven successful in revealing minute details from small-sized specimens from the same area with analogous preservation (Foffa et al., 2020; Keeble & Benton, 2020). Indeed, μCT offers the possibility to fully explore these specimens, reaching the smallest cavities and unprepared parts of the skeletons, permits virtual manipulation of the digital peels, helps verify the continuity of elements across slabs (and on different sides of the casts), as well as allowing the isolation, accurate measurement and visualization of individual bones (Figures 1 and 2). These new data allowed us to access and describe many previously unknown features and to rectify previous interpretations based on incomplete casts (see Section 4.1; Table 1). Finally, we illustrate and make freely available the digital models derived from these μCT data, which are currently the most complete and reliable source of information on this taxon and provide durable substitutes for the deteriorating historic casts and peels.

1.1 | Anatomical abbreviations

aeg, anterior extensor groove; **aof**, antorbital fossa; **as**, astragalus; **asf**, astragalus facet; **ast**, astragalar tuber; **c**, carpal; **ca**, calcaneum; **cat**, calcaneal tuber; **co**, coracoid; **ctf**, crista tibiofibularis; **d**, dentary; **dpc**, deltopectoral crest; **emf**, external mandibular fenestra; **en**, external naris; **fe**, femur; **fi**, fibula; **h**, humerus; **hh**, humeral head; **hy**, hyoid; **il**, ilium; **j**, jugal; **lco**, lateral condyle; **le**, lateral emargination; **lj**, lower jaw; **ma**, manus; **mc**, metacarpal; **mco**, medial condyle; **mt**, metatarsal; **mx**, maxilla; **na**, nasal; **oc**, occipital condyle; **op**; olecranon process; **or**, orbit; **pap**, preacetabular process; **ph**, phalanx; **pmx**, premaxilla; **poz**, postzygapophysis; **ppp**, prepubic peduncle; **prz**, prezygapophysis **pt**, pterygoid; **pu**, pubis; **q**, quadrate; **r**, rib; ra, radius; **rap**, retroarticular process; **sc**, scapula; **sk**, indeterminate skull fragments; **t**, tarsal; **ti**, tibia; **u**, ungual; **ul**, ulna; **4t**, fourth trochanter.

1.2 | Institutional abbreviations

BNM, Bündner Naturmuseum, Chur (Switzerland); **GR**, Ghost Ranch Ruth Hall Museum of Paleontology, Abiquiú, NM (USA); **NHMUK**, Natural History Museum, London (UK); **NMQR**, National Museum, Bloemfontein (South Africa); **PVL**, paleontological collection of the Fundación-Instituto Miguel Lillo, Universidad Nacional de Tucumán (Argentina); **TMM**, Vertebrate Paleontology Laboratory, Texas Natural Science Center, Austin, TX (USA); **UFRGS**, Paleovertebrate Collection of the Universidade Federal do Rio Grande do Sul, Rio Grande do Sul (Brazil); **ULBRA**, Centro de Apoio à Pesquisa Paleontológica da Quarta Colônia/Universidade Federal de Santa Maria, São João do Polêsine, Rio Grande do Sul,

Brazil (previously Museu de Ciências Naturais, Universidade Luterana do Brasil, Canoas, Brazil).

2 | METHODS

2.1 | µCT scanning methods

As reported by Foffa et al. (2022), all six specimens referred to *Scleromochlus taylori* (the holotype NHMUK PV R3556, NHMUK PV R3557, NHMUK RV R3146, NHMUK PV R3914, NHMUK PV R4823/4, and NHMUK PV R5589) were subjected to µCT scanning. The multiple sandstone blocks, in which each specimen is embedded were re-assembled and held together using rubber bands before µCT scanning (Figure 1c). This extra step ensured that each complete specimen fitted within a single scan in its "natural" association, minimizing the risk of misidentification of elements that are partly preserved in different slabs, and also improved measurement accuracy (Foffa et al., 2020, 2022; Figures 1 and 2). NHMUK PV R3557, was scanned at the Palaeobiology Lab of the University of Bristol, using a Nikon XT H 225 by Dr Tom G. Davis, assisted by Dr Elizabeth G. Martin-Silverstone; the other five specimens (NHMUK PV R3556, NHMUK RV R3146, NHMUK PV R3914, NHMUK PV R483/4, and NHMUK PV R5589) were scanned at the Imaging and Analyses Centre of the NHMUK, using the Nikon XT H 225 by Dr Vincent Fernandez with the assistance of PMB. The µCT data, scanning parameters, digital models of peels and new data are freely available at via Morpho-Source at: https://www.morphosource.org/projects/000414456/?locale=en (Foffa et al., 2022), following the recommendations of Davies et al. (2017).

2.2 | Phylogenetic methods

To test the phylogenetic relationships of *Scleromochlus taylori* we updated the dataset of Foffa et al. (2022)—which is a modified version of the matrix of Ezcurra, Jones, et al. (2020) (originally derived from Ezcurra (2016))—with the additional inclusion of the putative basal pterosauromorph *Maehary bonapartei* (but see Section 5, below, and the revised scorings and phylogenetic placement in Müller et al., 2023), the lagerpetid *Faxinalipterus minimus* (Kellner et al., 2022), and the Late Triassic pterosaurs *Pachagnathus benitoi* and *Yelaphomte praderioi* (Martínez et al., 2016, 2022). Due to its completeness and character sampling, the Ezcurra, Jones, et al. (2020) matrix is ideal for testing the phylogenetic affinities of *Scleromochlus*. All ambiguous ankle characters of *Scleromochlus taylori* (i.e., Chars. 532–562 and

Chars. 811–818) were left as "?," as recommended by Foffa et al. (2022).

The final dataset includes 822 characters and 162 active terminal taxa. The 36 most problematic or undiagnostic terminal units were excluded a priori from the analyses. These are: *Dinocephalosaurus orientalis*, *Fuyuansaurus acutirostris*, *Pectodens zhenyuensis*, *Protanystropheus antiquus*, *Trachelosaurus fischeri*, *Tanystropheus haasi*, *Malerisaurus robinsonae*, *Arctosaurus osborni*, *Eorasaurus olsoni*, *Prolacertoides jimusarensis*, *Archosaurus rossicus* (complete), *Panchet proterosuchid*, *Vonhuenia fredericki*, *Chasmatosuchus rossicus* (combined), *Chasmatosuchus magnus* (combined), *Chasmatosuchus vjushkovi*, *Koilamasuchus gonzalezdiazi*, *Kalisuchus rewanensis* (holotype), NMQR 3570, *Shansisuchus kuyeheensis*, *Uralosaurus* (combined), *Osmolskina czatkoviensis*, *Osmolskina* (complete), *Triopticus primus*, *Angistorhinus talainti*, "Otter Sandstone Formation Archosaur," *Dagasuchus santacruzensis*, *Hypselorhachis mirabilis*, "Waldhaus poposauroid," *Vytshegdosuchus zbeshartensis*, *Bystrowisuchus flerovi*, *Bromsgroveia walkeri*, "Moenkopi Formation poposauroid," *Lutungutali sitwensis*, and *Nyasasaurus parringtoni* (see Butler et al., 2019; Ezcurra, 2016; Ezcurra & Butler, 2018; Ezcurra et al., 2017; Ezcurra, Nesbitt, et al., 2020, for the reasons behind these exclusions). *Petrolacosaurus kansensis* was set as the outgroup. The following characters were treated as additive: 1, 2, 7, 10, 17, 19–21, 28, 29, 36, 40, 42, 46, 50, 54, 66, 71, 74–76, 122, 127, 146, 153, 156, 157, 171, 176, 177, 187, 202, 221, 227, 263, 266, 278, 279, 283, 324, 327, 331, 337, 345, 351, 352, 354, 361, 365, 370, 377, 379, 386, 387, 398, 410, 414, 424, 430, 435, 446, 448, 454, 455, 458, 460, 463, 470, 472, 478, 482, 483, 485, 489, 490, 502, 504, 510, 516, 521, 529, 537, 546, 552, 556, 557, 567, 569, 571, 574, 581, 582, 588, 636, 648, 652, 662, 701, 731, 735, 737, 738, 743, 749, 766, 784, and 816.

2.2.1 | Maximum parsimony analysis

The maximum parsimony analyses (equally weighted) were performed in TNT v. 1.5 (Goloboff et al., 2008; Goloboff & Catalano, 2016). We followed the same protocols given in Ezcurra, Nesbitt, et al. (2020) and Foffa et al. (2022) to search for the most parsimonious trees (MPTs): initial trees were found using the "Driven Search" option in the New Technology menu (Sectorial Search, Ratchet, Drift, and Tree fusing were left on default settings) until 100 optimal hits were reached. This procedure serves to broadly sample tree space. The most parsimonious trees were then subjected to an additional round of tree bisection reconnection branch swapping, which serves to explore the tree space in finer detail.

Consistency index (CI) and retention index (RI) were calculated using the script statsB.run (Spiekman et al., 2021), which automatically excludes deactivated terminals. Branch support was calculated using Bremer support values and bootstrap resampling, the latter with 1000 technical pseudo-replicates for both absolute and group present/contradicted (GC) frequencies.

2.2.2 | Bayesian inference analysis

We also conducted Bayesian tip-dating analysis using MrBayes (v. 3.2.7; Ronquist et al., 2009) with the same settings as the unconstrained analyses of Ezcurra, Nesbitt, et al. (2020) and Foffa et al. (2022). We ran a Markov k-state variable substitution with no topological constraint on the topology of the tree, and some time constraints to selected nodes: we implemented uniform age priors and gamma-rate relaxed clock models on First and Last Appearance Dates for all tips of the tree; the oldest split of the tree was set at 304.4–318 Mya based on the estimated age of *Petrolacosaurus kansensis* and the earliest occurrence of crown-amniotes in the Joggins Formation (Benton et al., 2015); the node age calibration of Archosauria was set at 249.2–257.4 Mya (uniform prior), based on the earliest occurrence of archosaurs in the fossil record, and the estimated age of the archosaur–squamate split (see Ezcurra et al., 2014, 2017). All tips were set to be fossils, in a fossilized birth–death process under standard parametrization. We used a Metropolis-coupling Markov chain Monte Carlo algorithm, two runs of four chains each with three swap attempts per generation and a heat coefficient of 0.05.

3 | SYSTEMATIC PALEONTOLOGY

Archosauria Cope, 1869
Avemetatarsalia Benton, 1999
Ornithodira Gauthier, 1986
Pterosauromorpha Padian, 1997
Lagerpetidae Arcucci, 1986
Scleromochlus taylori Woodward, 1907

3.1 | Holotype

NHMUK PV R3556, an almost complete impression of a skeleton in sandstone, currently split into four blocks. Some additional elements (pedal phalanges, ribs, and caudal vertebrae) are only visible in μCT scans and remain completely encased within the sandstone matrix.

3.2 | Referred material

NHMUK PV R3557, NHMUK PV R3146 (two individuals), NHMUK PV R3914, NHMUK PV R4823/4, NHMUK PV R5589, all of which are partial to complete impressions of skeletons preserved in sandstone in a similar fashion to the type specimen, and with variable numbers of elements still encased within the sandstone matrix.

3.3 | Locality and horizon

Lossiemouth East Quarry, Lossiemouth, near Elgin (Moray, Scotland, UK), with the exception of NHMUK PV R5589, which was recovered from the West Quarry of the same location.

3.4 | Stratigraphy

All the specimens come from the eolian sandstone deposits of the Lossiemouth Sandstone Formation (Upper Triassic: ~late Carnian/early Norian; see Benton, 1999; Benton & Walker, 1985, Benton & Walker, 2002; Ezcurra et al., 2017, Ezcurra & Butler, 2018, Ezcurra, Jones, et al., 2020, Langer et al., 2018) for comments on the biostratigraphic correlations of the Lossiemouth Sandstone Formation with other Upper Triassic formations.

3.5 | Diagnosis

Following Foffa et al. (2022), *Scleromochlus taylori* is a small-bodied, gracile lagerpetid avemetatarsalian with the following unique combination of character states (autapomorphies denoted by an asterisk): *retroarticular process of the mandible moderately expanded posteriorly, with a distal end that is weakly expanded dorsolaterally-to-ventromedially; *parietal with a transverse posterolateral process; anterior cervical with transversely convex ventral surface; *middle and posterior dorsal vertebrae with an elongated centrum (height/length ratio >2.5); straight (i.e., not sigmoidal) humerus; gracile humerus (present in some trees) with a maximum proximal transverse width /total length ratio ~ 0.16–0.2; *short deltopectoral crest, reaching only 15%–18% of the humeral length; short pubis, <30% of the total length of the femur; narrow femur distal transverse width, ~11% of the total length; short metacarpal, <10% of the length for the humerus and only ~18% the length than the longest

metatarsals; metatarsals I–IV equal in length (shared with pterosaurs, but not lagerpetids).

4 | RESULTS

4.1 | Description

4.1.1 | General remarks

The specimens of *Scleromochlus* have been discussed by numerous authors and their descriptions of the material are, in general, broadly accurate (Bennett, 1996, 2013, 2020; Benton, 1999; Broom, 1913; Gauthier, 1986; Martin, 1983; Padian, 1984; Sereno, 1991; Swinton, 1960; von Huene, 1914; Woodward, 1907). We use this section to expand upon the descriptions provided in Foffa et al. (2022), with an emphasis on rectifying previously misinterpreted features and reporting novel observations, and we provide additional comparisons and discuss how our new μCT data update past interpretations of *Scleromochlus* osteology.

The skeletons of all the available *Scleromochlus* specimens—and those of the other middle-to-small-sized taxa from the Late Triassic Elgin deposits (see Foffa et al., 2020)—have undergone diagenetic flattening. Some specimens are more severely distorted than others, with the distortion affecting both entire skeletons and individual elements (i.e., flattening of individual bones; e.g., NHMUK PV R3146). In some specimens, the bones are only minimally distorted, if at all (e.g., NHMUK PV R3556, NHMUK PV R3557), but the articulation relationships were modified post-mortem (e.g., collapse of the rib cage, disarticulation of limbs), presumably due to the fragility or small size of these structures. There are no preserved specimens in which the dorsoventral proportions of the skull or torso accurately represent their proportions and orientations in vivo (*contra* Bennett, 2020). Therefore, even though some skeletons appear to be in full articulation, their joints cannot be considered in life position, and should not be used to estimate their original ranges of motion. In many skeletons, there are instances of isolated bones that are disarticulated, indicating post-mortem disturbance (Foffa et al., 2022).

4.1.2 | Skull

The best-preserved skulls are those of NHMUK PV R3556, NHMUK PV R3557, and NHMUK PV R3146, with additional details available from NHMUK PV R3914. The skull is roughly triangular in dorsal view, with the snout (pre-orbital length) making up ∼50% of its total length

(Figures 2–4a). Several authors considered the skull of *Scleromochlus* to be dorsoventrally flattened in life (Bennett, 2020; Benton, 1999); however, we find no evidence in support of this hypothesis, and skull flattening is likely linked to taphonomic processes (Foffa et al., 2022). It is not possible, with the information available, to determine whether the skull was wider transversely tall dorsoventrally or vice versa, but we consider the former option unlikely as it would be an unusual condition among avemetatarsalians. Similarly, it is impossible to determine whether the premaxillae of *Scleromochlus taylori* formed a beak, as recently reported for *Venetoraptor gassenae* (Müller et al., 2023) and other basal avemetatarsalians (i.e., silesaurids; Dzik, 2003; Nesbitt et al., 2020), dinosaurs (e.g., Zanno & Makovicky, 2011), and shuvosaurid pseudosuchians (e.g., Nesbitt & Norell, 2006).

Sutures are not clearly visible in any of the available skull specimens (in either the real specimens, peels, or digital data). Historically, the inability to verify the continuity of cranial bones seen separately in the dorsal and ventral peels has resulted in debates on the identifications of some cranial elements (e.g., the maxilla). This issue particularly affects NHMUK PV R3556, NHMUK PV R 3557, and NHMUK PV R3146. For instance, μCT models support Bennett's (2020) interpretation of the skull of NHMUK PV R3146 over Benton's (1999) (Figures 2c and 3e–i). The maxilla, not the dentary (*contra* Benton, 1999), is exposed in the left side of the dorsal view, and next to the left mandibular ramus in ventral view (see fig. 6, Bennett, 2020). In other words, the mandible of this specimen is not visible on the dorsal peel, while the maxilla is exposed on the ventral one (Figures 2c and 3e–i).

Another debated feature is the presence (Benton, 1999; Sereno, 1991) or absence (Bennett, 2020) of an antorbital fossa, and its extent on the ventral, anterior, and lateral borders of the maxilla. The μCT scans show that an antorbital fossa is preserved in four specimens: NHMUK PV R3556, NHMUK PV R3557, and NHMUK PV R3146 (both individuals) (Figures 3a,c,e and 4a), and extends onto the anterior and lateral sides of the maxilla, but it is impossible to determine how far it extends posteriorly. By contrast, the antorbital fossa is restricted to the dorsal process in *Maehary bonapartei* (CAPPA/UFSM 0300; Kellner et al., 2022). The antorbital fossa of *Scleromochlus taylori* is particularly well exposed in NHMUK PV R3556, NHMUK PV R3557, and NHMUK PV R3146, and the anterodorsal process of the maxilla frames its anterior margin (Figures 3 and 4). This process is well-developed dorsally and posteriorly curved in NHMUK PV R3556 and NHMUK PV R3557, as shown by the μCT data. The dorsal extent of this process, and the clear collapse of the premaxilla and nasal in between, is additional evidence against the notion of a dorsoventrally flattened skull in *Scleromochlus*. The anterior border of the
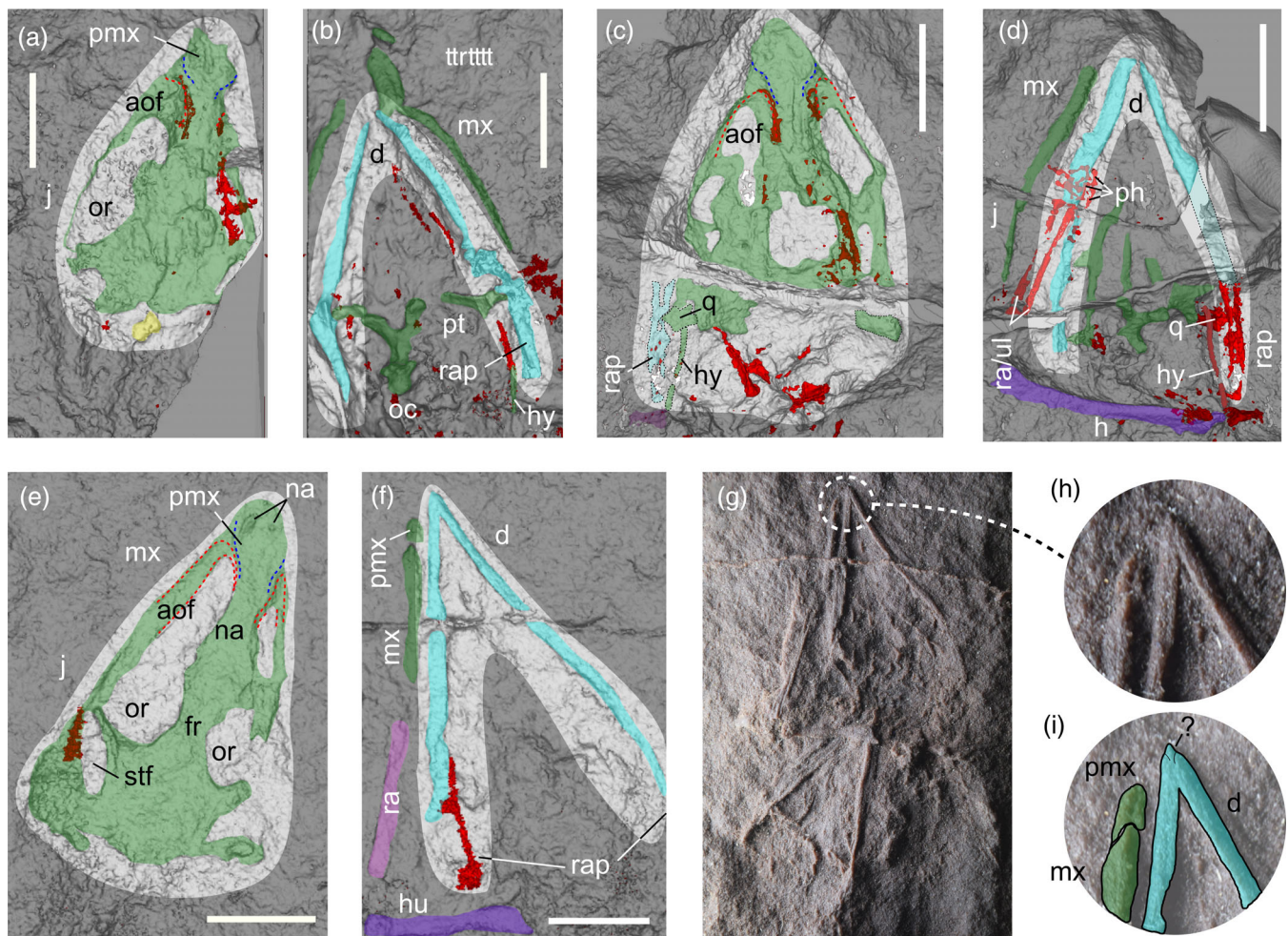
FIGURE 3   Details of *Scleromochlus taylori* skulls. (a,b) NHMUK PV R3556 in dorsal (a), and ventral (b) views. (c,d) NHMUK PV R3557 in dorsal (c) and ventral (d) views. (e,f) NHMUK PV R3146, digital peels of "individual A" in dorsal (e) and ventral (f) views. (g–i) PVC cast of the ventral slab. The blue dashed line indicates the premaxilla-maxilla suture, and the red dashed line indicates the identifiable border of the antorbital fossa. Scale bars equal 10 mm. See the main text for abbreviations.

maxillary anterodorsal process is weakly concave (with an anteriorly directed concavity, visible in NHMUK PV R3146 and NHMUK PV R3557; Figures 3a,c,e and 4a). The maxillary anterior process tapers anteriorly and has a weakly concave dorsal margin, a state that *Scleromochlus* shares with *Maehary bonapartei* (CAPPA/UFSM 0300), Lagerpetidae and Pterosauria (Ezcurra, Nesbitt, et al., 2020; Foffa et al., 2022; Kammerer et al., 2020; Kellner et al., 2022). It is not clear whether the maxillae contributed to the margins of the external nares, as in early pterosaurs and potentially *Kongonaphon* and *Ixalerpeton* (Ezcurra, Nesbitt, et al., 2020; Kammerer et al., 2020), or not, as in *Maehary bonapartei* (CAPPA/UFSM 0300; Kellner et al., 2022). The position of the external nares can be seen in the peel of the premaxillary area of NHMUK PV R3557 (Figures 3c,e and 4a). The parietal has transversely oriented processes (NHMUK PV R3146) that, following the Foffa et al.'s (2022) phylogenetic analyses, are regarded as an autapomorphy of *Scleromochlus*.

The µCT data from NHMUK PV R3557 reveal rarely seen details of the posterior part of the skull. The posterior and distal parts of the left quadrate are preserved in close proximity to the posterior end of the left mandibular ramus and the left hyoid bone (Figures 3c,d and 4a–d; Foffa et al., 2022). Similarly, parts of the right lateral cranium (maxilla, jugal, quadrate?) are preserved in NHMUK PV R3914, associated with the right forelimb and the posterior half of the right lower jaw (Figure 4e,f). Based on these data, the morphology and orientation of the quadrate can be reconstructed confidently. The posterior surface of the quadrate is straight and the bone is posteriorly oriented in lateral view (Bennett, 2020; Foffa et al., 2022). This observation rectifies previous descriptions, which incorrectly showed *Scleromochlus taylori* with an anteriorly inclined quadrate (Benton, 1999), a feature that, being common in pterosaurs (Dalla Vecchia, 2013), was used previously to support a close
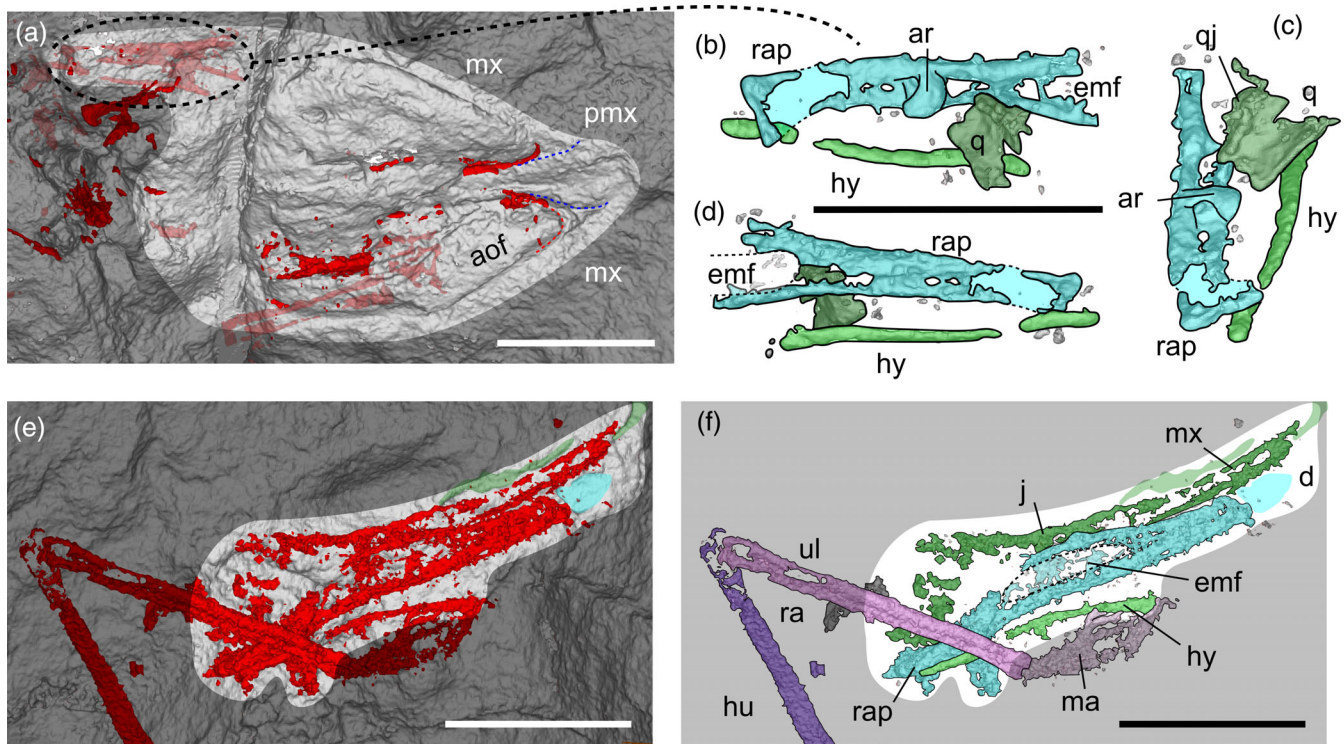
FIGURE 4 New details of *Scleromochlus taylori* skulls from µCT scans. (a–d) NHMUK PV R3557. (a) Skull in right dorsolateral view; (b–d) quadrate, retroarticular process and hyoid bone in dorsomedial (b), dorsoposterior (c), and ventrolateral (d) views. (e,f) NHMUK PV R3914, right forelimb and posterior side of the right side of the skull and lower jaw in ventrolateral view. The blue dashed line in b indicates the premaxilla-maxilla suture, and the red dashed line indicates the anterior border of the antorbital fossa. Scale bars equal 10 mm. See main text for abbreviations.

relationship between these taxa. The posterior surface of the left quadrate of NHMUK PV R3557 is very weakly concave, as is common among archosauromorphs (Ezcurra, 2016), and similar to the condition in *Maehary bonapartei* (CAPPA/UFSM 0300) (Kellner et al., 2022). It is not deeply excavated (i.e., a quadrate conch is absent), thereby lacking a feature considered to be diagnostic of lepidosauromorphs, such as *Brachyrhynodon taylori* and *Planocephalosaurus robinsonae* (Ezcurra, 2016; Fraser & Benton, 1989; Gauthier et al., 1988). The ventral quadrate condyles of NHMUK PV R3557 are equally extended distally, as also occurs in most other diapsids (Ezcurra, 2016).

In the braincase, the basal tubera are present and well exposed in NHMUK PV R3556 and NHMUK PV R3557. They are rounded, diverge from each other and are clearly separated. The basioccipital neck is very short, as also occurs in lagerpetids and basal pterosaurs (Ezcurra, Nesbitt, et al., 2020; Figures 3b and 5a).

Tooth counts for the premaxilla and maxilla are currently impossible to assess based on the preserved specimens. Based on the shape of the alveoli in NHMUK PV R3557, we concur with Bennett (2020) that the teeth were likely mediolaterally compressed, in contrast to those of

Maehary bonapartei and other lagerpetids that possess more circular cross-sections (Ezcurra, Nesbitt, et al., 2020; Kellner et al., 2022). We find it unlikely that this taxon had vomerine, palatine, or pterygoid teeth. It is possible, however, that these structures, if originally present, might have been too small to be detected in *Scleromochlus* (as they could have been smaller than the resolution of the digital data or the individual grain sizes of the sandstone) (see suppl. inf. in Foffa et al., 2020); therefore, the corresponding character states were scored cautiously as "?." Indeed, such palatal teeth are present on the rostral process of the pterygoid of *Maehary bonapartei* (Kellner et al., 2022).

4.1.3 | Lower jaw

The lower jaw of *Scleromochlus* is best known from peels taken from the ventral slabs of NHMUK PV R3556, NHMUK PV R3557, and NHMUK PV R3146. The interpretation of the lower jaw has been controversial, partly because of disagreement about which parts of the mandible are visible on the peels of the ventral slab of NHMUK PV R3556. Based on µCT scans and continuity between
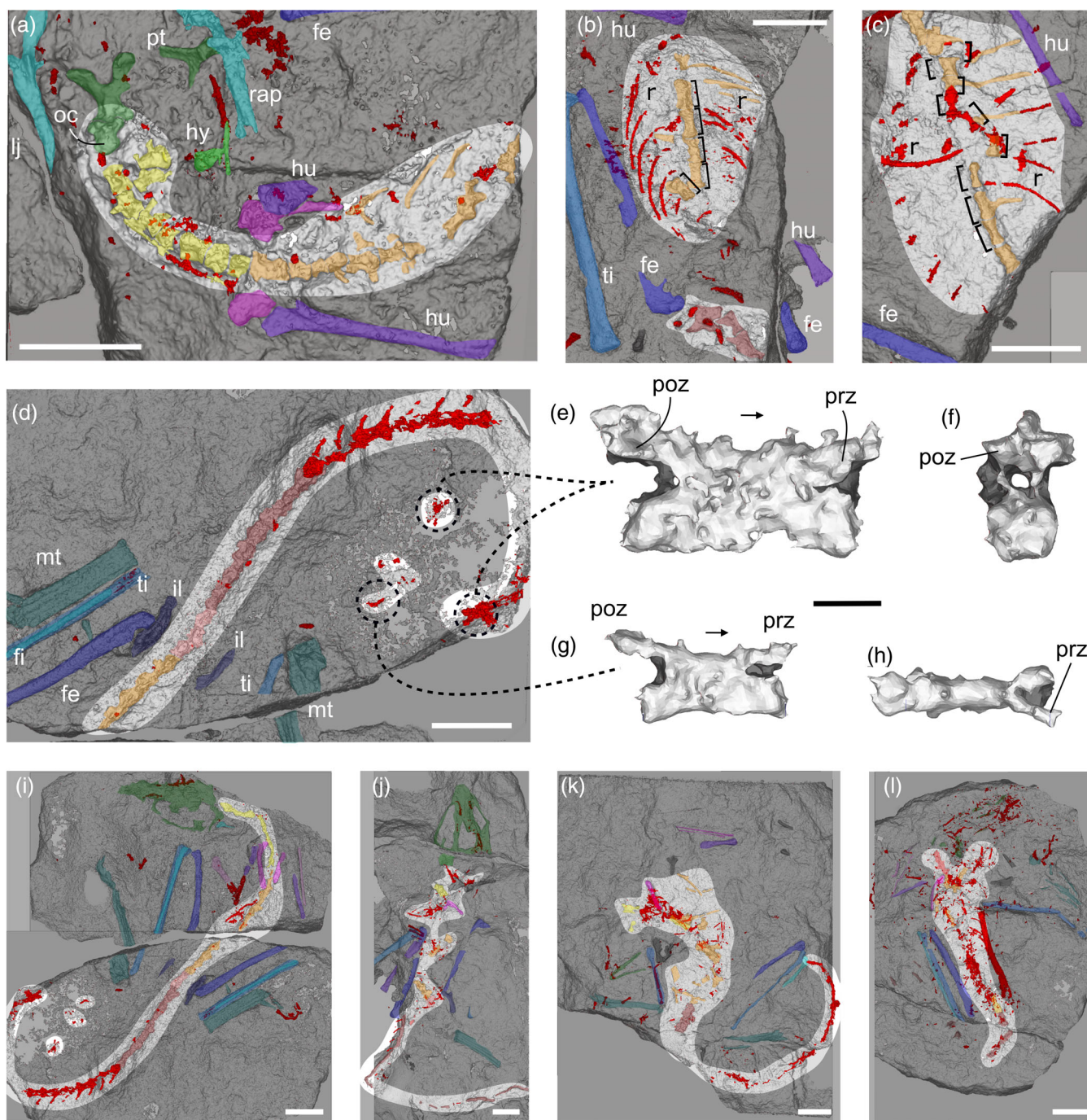
FIGURE 5 Vertebral columns of *Scleromochlus taylori* specimens from μCT scans. (a) NHMUK PV R3556, posterior skull, mandible, cervical and dorsal vertebral series, and ribcage in ventral view. (b) NHMUK PV R3557, dorsal and anterior caudal series in ventral view. (c) NHMUK PV R3914, anterior and middle dorsal vertebral series and ribcage in ventral view. (d) NHMUK PV R3556, posterior dorsal, sacral and caudal vertebral series in dorsal view. (e,f) NHMUK PV R3556, posterior caudal vertebra in lateral (e) and posterior (f) views. (g,h) NHMUM PV R3556, posterior caudal vertebra in lateral and dorsal view. (i) NHMUK PV R3556 skeleton in dorsal view. (j) NHMUK PV R3557 skeleton in dorsal view. (k) NHMUK PV R5589 skeleton (uncertain view). (l) NHMUK PV R4823/4 skeleton in dorsal view. Scale bars equal 10 mm in a–d, i–l and 1 mm in e–h. See main text for abbreviations.

the dorsal and ventral sides, we confirm that the interpretation of Bennett (2020) should be preferred over that of Benton (1999) for this specimen (Figure 3b). In ventral view, the lower jaw of *Scleromochlus* is nearly identical to

those of *Ixalerpeton polesinensis* (ULBRA-PVT059) and *Lagerpeton chanarensis* (PVL 4265; Ezcurra, Nesbitt, et al., 2020). There is no clear indication that the anterior part of the lower jaw of *Scleromochlus* is ventrally

deflected as in other lagerpetids (Ezcurra, Nesbitt, et al., 2020), with the exception of a weak curvature in NHMUK PV R3146 and NHMUK PV R3557 that might be a preservational artefact. The dentary symphysis is very short and positioned entirely within the anterior quarter of the lower jaw as seen in NHMUK PV R3556, NHMUK PV R3146 (Figure 3) and *Maehary bonapartei* (CAPPA/UFSM 0300) (Kellner et al., 2022). The anterior end of the mandible in NHMUK PV R3146A tapers anteriorly in ventral view (Figure 3f–i), suggesting that the anterior-most tip might have been edentulous (Foffa et al., 2022), as also occurs in *Ixalerpeton polesinensis* (ULBRA-PVT059) and *Lagerpeton chanarensis* (PVL 4265), early pterosaurs, such as *Seazzadactylus venieri* (MFSN 21545), *Carniadactylus rosenfeldi* (MFSN 1797), and *Raeticodactylus filisurensis* (BNM 14524), and silesaurids (e.g., *Silesaurus opolensis* [ZPAL Ab III/361]; *Asilisaurus kongwe*; Cabreira et al., 2016; Dalla Vecchia, 2013, 2014, 2019; Dzik, 2003; Ezcurra, Nesbitt, et al., 2020; Langer et al., 2013; Nesbitt et al., 2020). However, without a clear dorsal or lateral view of this area this feature cannot be confirmed. Not all pterosauromorphs have an edentulous anterior dentary, however, as in *Maehary bonapartei* (CAPPA/UFSM 0300) it bears teeth (Kellner et al., 2022).

The external mandibular fenestra is another highly debated feature. The presence of a fenestra was implied, but never overtly discussed, by some authors (Benton, 1999; von Huene, 1914), and denied by others (Bennett, 2020; Sereno, 1991). Newly segmented posterior fragments of the mandibular rami in NHMUK PV R3557 and NHMUK PV R3914 demonstrate unequivocally that *Scleromochlus taylori* had a well-developed external mandibular fenestra, but its precise size remains unclear. Its anterior extent is tentatively estimated to be one-third of the length of the portion of the dentary anterior to the fenestra itself (Figure 4). Previously, the absence of an external mandibular fenestra was used to support a close relationship between *Scleromochlus* and pterosaurs (Sereno, 1991). However, this argument is no longer tenable as both *Scleromochlus* and the early pterosaur *Austriadactylus dellavecchiai* (SMNS 56342) have been shown to possess an external mandibular fenestra (Dalla Vecchia, 2021; Kellner, 2015; Nesbitt & Hone, 2010). This indicates that an external mandibular fenestra is likely plesiomorphic in Pterosauromorpha, seeing as it is a broader archosauromorph character, and that it may have been lost in more nested pterosaurs instead.

New data from NHMUK PV R3556, NHMUK PV R3557, and NHMUK PV R3914, and the reinterpretation of the peels of NHMUK PV R3556 and NHMUK PV R3146, show that the retroarticular process was long, as interpreted by Benton (1999). The same feature was interpreted by Bennett (2020) as a crack in the block of NHMUK PV R3556, but μCT data show that while a crack is present, the right retroarticular process is also present and well-developed to project beyond the glenoid fossa, mirroring in length and proportions the newly segmented posterior jaw on the left mandibular ramus. This area is better preserved in NHMUK PV R3557 and NHMUK PV R3914, both of which reveal that the posterior end of the retroarticular process is also moderately expanded in oblique direction (Figure 4b–f).

Other features that characterize the lower jaws of pterosauromorphs cannot be examined in any *Scleromochlus* specimen and would require new, exceptionally preserved specimens to be assessed. These include: the absence of the splenial (absent in *Lagerpeton chanarensis* [PVL 4265] and reduced or fused in pterosaurs); a high tooth count; the presence of multi-cusped teeth; and absence of interdental plates (Ezcurra, Nesbitt, et al., 2020).

4.1.4 | Axial column

The neck of *Scleromochlus* is short, composed of eight (or nine) vertebrae, which are best observed in NHMUK PV R3556 (ventral slab) (Figure 5a). The cervical vertebrae of *Scleromochlus* do not change significantly in length along the cervical series, as already noted (Bennett, 2020; Sereno, 1991). The neck is short overall in comparison to both skull and trunk lengths (Bennett, 2020; Benton, 1999) and constitutes only a minor percentage (∼30%) of the presacral column length (Figures 2 and 5). The short cervical centra of *Scleromochlus* result in a neck that is comparatively shorter than those of most pterosaurs, aphanosaurs, and other early avemetatarsalians (Nesbitt et al., 2017; Yáñez et al., 2021). It is unclear whether the neck of *Scleromochlus* had the "S-shaped curve" characteristic of most avemetatarsalian clades (Gauthier, 1986).

The very small size of the specimens coupled with their preservation and the resolution of the μCT scans make finer details of each vertebra (laminae, foramina, depressions) nearly impossible to assess. Nonetheless, other important details can be added to previous descriptions. For instance, the ventral surfaces of the cervical centra are transversely convex. The ribs on the cervical vertebrae are dicephalous, thin, and moderately short (less than the length of two consecutive centra) with a shaft that extends parallel to the main axis of the neck (Figure 5a). No depressions, fossae or foramina are observable, even in the better-preserved vertebrae of NHMUK PV R3556 and NHMUK PV R5589, but some

of these features might be too small to be clearly detected, even in the μCT scans.

The trunk of *Scleromochlus* is composed of ~15 vertebrae. The lengths of the anterior dorsal centra are comparable to those of the posterior cervicals and both are visibly shorter than the posterior dorsals (*contra* Bennett, 2020; Figure 5a,c). Specifically, the middle and posterior dorsal centra are exceptionally long in comparison to those of other archosaurs, with the centrum being more than twice as long as it is tall. This feature can be seen clearly in NHMUK PV R3556, NHMUK PV R3557, NHMUK PV R4823/4 and, particularly well, in NHMUK PV R3914, where the centrum length vs height ratio exceeds ~2.5 in the posterior dorsals (Figures 2a–c and 5). This condition is brought to an extreme in *Scleromochlus* that is unmatched in other Triassic archosaurs (see tab. 4 in Padian, 2008), although some coelophysoid theropod dinosaurs (e.g., *Coelophysis bauri*, CM C-3-82) also have elongated dorsal centra (Colbert, 1989; Ezcurra & Cuny, 2007; Rauhut, 2003). Among archosauromorphs, only the tanystropheid *Macrocnemus bassanii* has comparably long (or even longer) dorsal centra (Dzik, 2003).

The elongation of the dorsal centra contributes to the unique body shape of *Scleromochlus*. The overall length of the dorsal series in *Scleromochlus* is long relative to that of pterosaurs, which have a diagnostically short trunk, presumably linked to changes in body mass distribution for flight efficiency. However, the proportions of *Scleromochlus* are more similar to taxa at the base of Avemetatarsalia, such as *Teleocrater rhadinus* (NHMUK PV R6795), other aphanosaurs, and *Silesaurus opolensis* (ZPAL Ab III/361) (Dzik, 2003; Nesbitt et al., 2017, 2020) also have elongated dorsal series. Comparing this feature with other lagerpetids is problematic due to their incompleteness, as *Ixalerpeton polesinensis* (ULBRA-PVT059) is the only known lagerpetid with a complete and articulated dorsal series (Cabreira et al., 2016). In *Ixalerpeton polesinensis* the dorsal series is approximately twice as long as the femur and 2.56 times the length of the humerus, even though the middle and dorsal centra are not as elongated as in *Scleromochlus*. By contrast, the dorsal series of *Scleromochlus* is only 1.5 times the length of the femur, and 2.10 times the length of the humerus, but this is likely due to the comparatively long limbs of *Scleromochlus*, rather than shortening of the trunk. Overall, when compared with hindlimb length, the length of the dorsal series in *Scleromochlus* is intermediate between that of most archosaurs and pterosaurs. These different proportions have interesting biomechanical implications related to the position of the center of mass, and may reflect differences in locomotory strategy, a possibility that will be explored in a separate study. The diapophyses and parapophyses of the dorsal vertebrae lie close to the midline, rather than on laterally expanded pedicels, and the transverse processes are short in the middle and posterior dorsal vertebrae. The neural spine is rectangular in lateral view, small in size, and displaced posteriorly between the zygapophyses.

The trunk of *Scleromochlus* is deeper than wide (Foffa et al., 2022) and similar to those of other avemetatarsalians and most archosaurs (except for Doswellidae) (Sues et al., 2013). Evidence for this body shape is the geometry of the long, curved thoracic ribs visible in the μCT scans of NHMUK PV R3557, NHMUK PV R4832/4, and NHMUK PV R3914 (Figures 2 and 5b,c). This contrasts with earlier studies that described the ribs of *Scleromochlus* as short, weakly curved (Benton, 1999) and mainly laterally oriented (Bennett, 2020), leading to suggestions that the trunk was dorsoventrally compressed (Bennett, 2020; Benton, 1999; Sereno, 1991; von Huene, 1914; Woodward, 1907). This incorrect interpretation undoubtedly derives from prior assumptions that the rib cage impressions on the peels of NHMUK PV R3146, NHMUK PV R3914, and NHMUK PV R3557 captured most of the total length of the dorsal ribs (Figures 1, 2, and 5b,c). However, we are able to show that the lengths, orientations, and shapes of these ribs were misinterpreted (Foffa et al., 2022). The μCT data of NHMUK PV R3556, NHMUK PV R3557, and NHMUK PV R3914 demonstrate that the rib lengths have been greatly underestimated, and that they continue within the matrix for at least three to four times the lengths captured by the peels (Figure 5b,c). The ribs of NHMUK PV R3557 and NHMUK PV R4823/4 are stacked onto each other (Figure 5b) in a manner that is indicative of post-mortem collapse and rotation of the ribcage. In NHMUK PV R3914 the ribs have been pushed away from the midline post-mortem (Figure 5c), and thus appear unnaturally articulated with the vertebrae. The observation that the torso of *Scleromochlus* was not dorsoventrally short and/or flattened (Bennett, 2020), but taller than wide, has important implications for reconstructing the mode of life of this taxon and argues against hypotheses of obligate quadrupedality and sprawling stance (Bennett, 2020). A series of fragmented ribs in close association with the middle dorsal region of NHMUK PV R4823/4 shows that the ribs had dicephalous attachments to the corresponding vertebrae (Figure 2).

The sacrum of *Scleromochlus* is reduced in size and was most likely composed of two sacral vertebrae, instead of three or four as suggested by earlier authors (Bennett, 2020; Benton, 1999; von Huene, 1914; Woodward, 1907). There is no positive evidence to indicate that more than two sacral vertebrae articulated with the ilium. NHMUK PV R5589 has expanded ribs in at least two vertebrae, but unfortunately this cannot be

verified in any other specimen, except perhaps one vertebra of NHMUK PV R3557. Based on the lengths of the centra and of the ilium, and on comparisons with the sacrum of _Lagerpeton_ and _Ixalerpeton_, we find it most likely that _Scleromochlus_ had two—and certainly no more than three—sacral vertebrae.

The length of the tail of _Scleromochlus_ has long been debated. Woodward (1907) and von Huene (1914) disagreed on the number of caudal vertebrae (51 and 62, respectively), but their reconstructions agreed that the tail was long (see tab. 3 in Bennett, 2020). Successive publications described or illustrated _Scleromochlus_ with an unusually short tail (see fig. 18 in Sereno, 1991; fig. 14 in Benton, 1999), with 25 or 35 vertebrae, respectively. Bennett (2020) recognized these errors and conservatively estimated >35 caudal vertebrae (based on the maximum number of vertebrae that could be counted in the peels). Additional vertebrae that were digitally isolated from the matrix of NHMUK PV R3556 and NHMUK PV R5589 demonstrate that the tail of _Scleromochlus taylori_ is unequivocally longer than depicted by Sereno (1991) and Benton (1999), and more consistent with earlier estimates by Woodward (1907) and von Huene (1914). Specifically, we counted a total ∼35 in NHMUK PV R3556, and ∼27 in NHMUK PV R5589, including isolated distal caudal vertebrae (Figure 5d,i–l). Due to long missing segments between the preserved portions of these tails, the original total vertebral count must have been significantly higher. The spacing between the preserved segments and the morphology of the preserved centra enable more accurate assessments of caudal vertebral count. Specifically, comparisons between the morphology of the preserved vertebrae (i.e., size, presence or absence and prominence of the neural spine and pre- and postzygapophyses) in these two specimens indicate that the segment preserved in NHMUK PV R5589 includes a more distal portion of the tail than that in NHMUK PV R3556 (Figure 5i,k). Similarly, a high number of vertebrae is supported by the faint marks attributed to the middle and posterior caudal vertebrae in the matrix of NHMUK PV R3557, already noted by Woodward (1907), von Huene (1914) and Benton (1999) (Figure 5j). Overall, estimates based on comparisons and morphological features of individual vertebrae show that the tail of _Scleromochlus_ was at least twice the length of the presacral vertebral column. Based on all of the available data, we estimate conservatively that the tail of _Scleromochlus_ had ∼50 vertebrae.

The centra of the caudal vertebrae are longer than those of the cervicals and anterior dorsals but are only slightly longer than those of the middle and posterior dorsals. Their length does not increase distally, in contrast to the condition seen in the Triassic pterosaur _Prenodactylus buffarini_ (MFSN 1770; Dalla Vecchia, 2013).

The centra of the anterior caudal vertebrae are nearly the same length as, or marginally longer than, the posterior ones (∼3 mm in C4 vs. 3.20 mm in ∼C30 of NHMUK PV R3556): this condition occurs in all specimens with reasonably well-preserved tails (i.e., NHMUK PV R3556; NHMUK PV R5589; Figure 5e–h). The μCT scans of NHMUK PV R3556 and NHMUK PV R3557 show that the transverse processes of the anterior caudal vertebrae are posterolaterally directed, and moderately wide. The neural spines of the anterior vertebrae are posteriorly inclined in NHMUK PV R3556, and their transverse processes/ribs are moderately laterally extended and their bases are positioned entirely on the anterior half of the centrum.

4.1.5 | Gastralia

Benton (1999) reported the presence of gastralia on the top part of NHMUK PV R4823/4. Here, we interpret these fragments as disarticulated and crushed parts of the skull—including two short, tooth-bearing elements. We did not find unambiguous gastralia in our μCT scan data, but numerous striations on the casts of NHMUK PV R3557, and isolated elements in other specimens, suggest that they were likely present (Figure 2).

4.1.6 | Pectoral girdle and forelimbs

Well-preserved elements from the pectoral girdles can be seen in NHMUK PV R3556 (scapula), NHMUK PV R3557 (partial coracoid and putative scapula), and NHMUK PV R3914 (coracoid and scapula), but incomplete elements are exposed in the other specimens (Figures 2, 5a, and 6). Complete forelimb elements can be found in most specimens, with very good partial views on the peels of NHMUK PV R3556, NHMUK PV R3557, NHMUK PV R3914, and NHMUK PV R4823/4, but only fragmentary or deeply distorted elements can be seen in NHMUK PV R3146 and NHMUK PV R5589 (Figure 2). The μCT scan data have revealed the presence of previously unknown, intact forelimb elements within the matrix of NHMUK PV R3914 and NHMUK PV R3557, including partially complete hands and scattered phalanges (Figure 7).

Scapula
The scapula is thin, strap-like and longer than previously reported. The ratio between the scapula and humerus length in _Scleromochlus_ (scapula length: humerus length ∼0.70) is lower than that in _Lagerpeton chanarensis_ (MCZ 101540) (∼0.83), but greater than previously
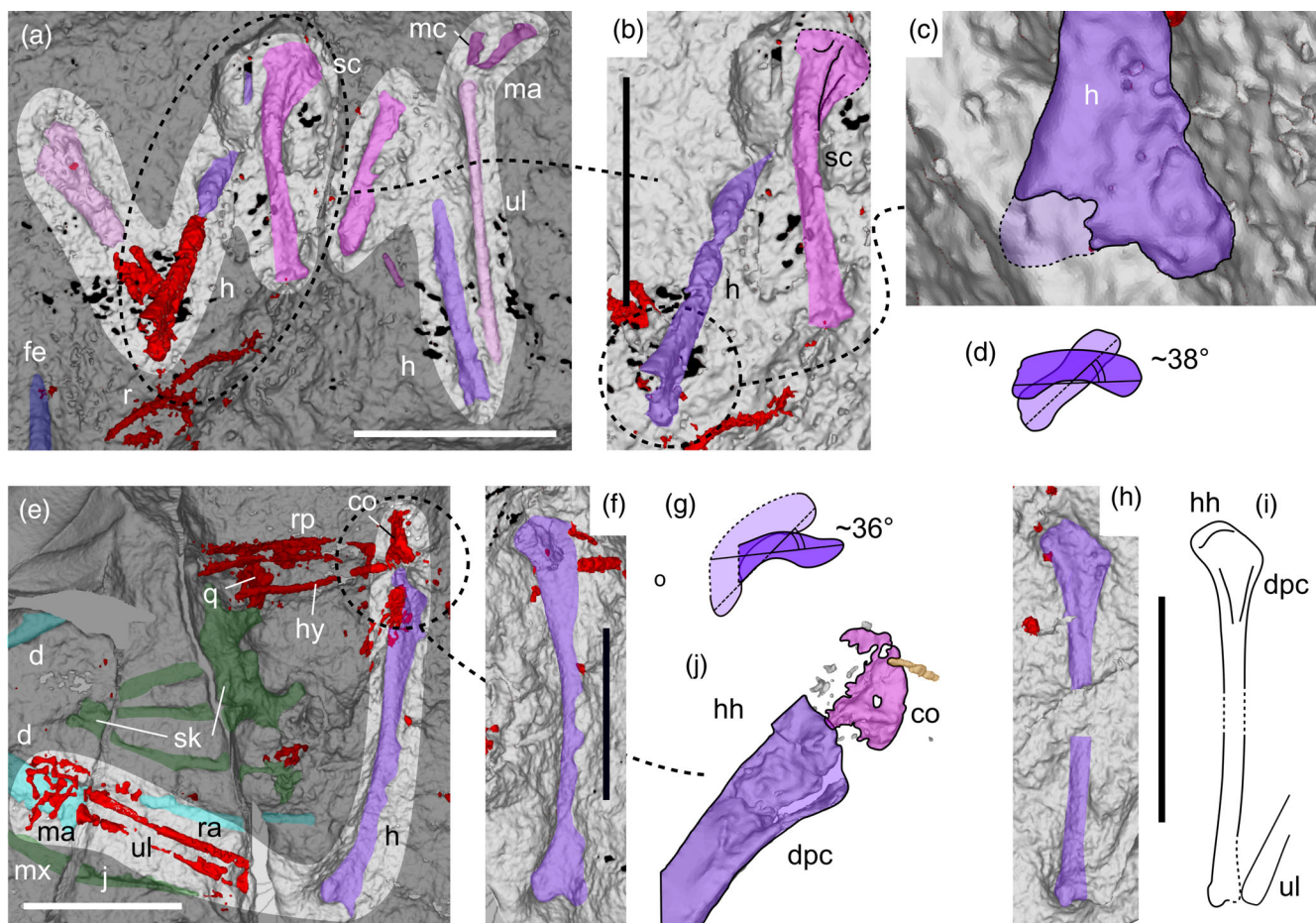
FIGURE 6 Shoulder girdle and forearm of *Scleromochlus taylori*. (a) NHMUK PV R3556 shoulder girdle and forelimb in dorsal view. (b) Detail of the left scapula and distal half of the left humerus in dorsal view. (c) Distal end of the humerus. (d,g) Interpretative drawings showing the relative orientation of the humeral head (dark) and distal end (light), proximal view of NHMUK PV R3556 (d), and NHMUK PV R3557 (g). (e) NHMUK PV R3557, skull and forelimb. (f) Humerus in medial view. (h,i) NHMUK PV R4823/4 left humerus in anterior view. (j) Detail of the humeral head and fragment of the coracoid NHMUK PV R3557. Digital rendering of the peels in grey; previously unavailable details are figured in bright red. Scale bars equal 10 mm. See main text for abbreviations.

thought (~0.56; reported by McCabe et al., 2021) and lower than that in most other archosaurs (McCabe et al., 2021). Padian (1984) and Sereno (1991) interpreted this ratio as evidence for a short scapula, which was regarded as a feature uniting pterosaurs and *Scleromochlus*. The scapula of *Scleromochlus* is, however, marginally longer than estimated by these authors, as previous studies could not account for the fact that the left humerus and scapula visible in the casts of NHMUK PV R3556 and NHMUK PV R3146, and the scapula of NHMUK PV R3146, are incomplete in the peels. The missing distal end of the left humerus in NHMUK PV R3556 is visible only in the μCT scans and shows that the humerus is ~18.5 mm long, and the scapula, which is partly exposed in both blocks, is ~13 mm long (Figure 6a,b). Although this does not drastically affect the ratio, it demonstrates that the scapula of *Scleromochlus* is not nearly as short as previously thought. This notion

is consistent with data from other specimens such as NHMUK PV R3914, NHMUK PV R4823/4, and NHMUK PV R5589, but not NHMUK PV R3146, where both the scapula and humerus are incompletely preserved. Our observations agree in general with those of Benton (1999). The overall proportions of this element are gracile (total length:minimum anteroposterior width ~10–11) and elongate with a weakly expanded distal end, which is broadened even less than that in *Ixalerpeton* (Cabreira et al., 2016; Ezcurra, Nesbitt, et al., 2020). The anterior margin of the scapula of *Scleromochlus* is concave (Figure 6a,b), as in lagerpetids and most avemetatarsalians, in contrast to those of pterosaurs, which have a scapula with a straight anterior margin, and to *Silesaurus opolensis* whose scapula has a convex anterior margin (Dzik, 2003). Overall, the scapula of *Scleromochlus taylori* is most similar to that *Dromomeron romeri* (GR 238) (McCabe et al., 2021).
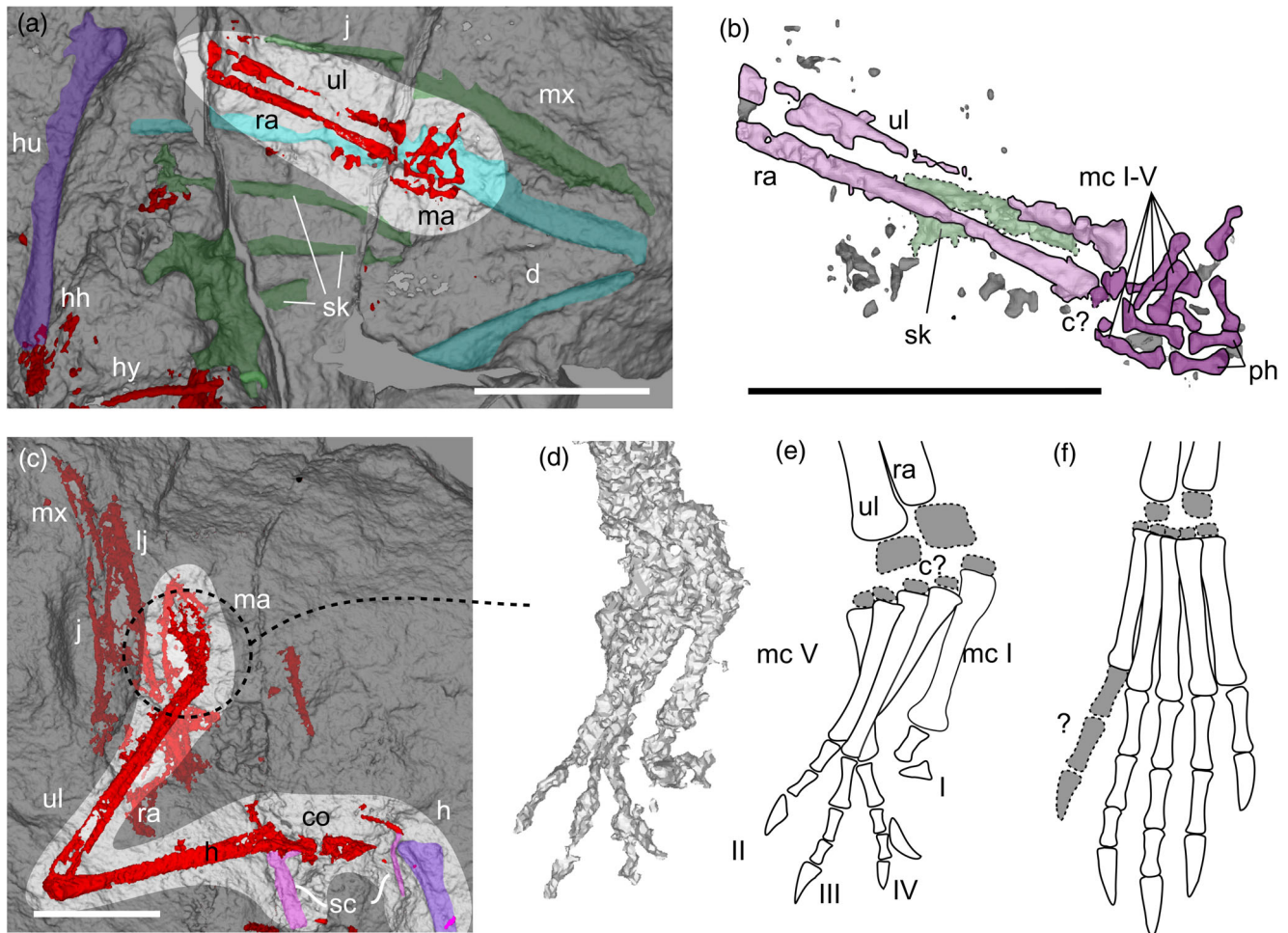
FIGURE 7 Forearm and manus of *Scleromochlus taylori*. (a) NHMUK PV R3557, right arm, posterior skull and mandible in ventral view. (b) NHMUK PV R3557, proximal forelimb and manus. (c) NHMUK PV R3914, right forelimb, shoulder girdle and skull. (d,e) NHMUK PV R3914, manus in dorsal oblique view and interpretative drawing. (f) reconstruction of the right manus of *Scleromochlus taylori* in dorsal view. Digital rendering of the peels in grey; previously unavailable details are figured in bright red. Scale bars equal 10 mm. See main text for abbreviations.

Coracoid

Fragments of both coracoids are associated with a complete forelimb in NHMUK PV R3914 (Figure 7c). Unfortunately, they are not well enough preserved to enable a detailed description (the anterior portions were lost during the historic breaking of the sandstone block), or to determine whether the coracoid is fused with the scapula, as occurs in other pterosauromorphs (Ezcurra, Nesbitt, et al., 2020). The medial and posterior parts of both coracoids have posterior concave margins and rounded medial margins (Figure 7c) and appear to be wider than tall. The putative coracoid described by Benton (1999) on the ventral peel of NHMUK PV R3556 lies in an area that was previously heavily prepared and altered in an attempt to obtain better casts, so we do not consider it a reliable source of information. The anterior part of the coracoid is preserved in NHMUK PV R3557 in proximity to the proximal end of the right humerus (Figure 7a). This fragment preserves part of the glenoid fossa, and an anteromedial margin that is clearly rounded and convex in accordance with the data from NHMUP PV R3914.

Humerus

The humerus of *Scleromochlus* has been described well by other authors, but we are able to reveal additional details relating to its proportions and distal end. Humeral length is 64%–69% of femoral length in all specimens (contrasting with the estimate of 60% in Benton, 1999, which was based primarily on peels of NHMUK PV R3556) (Figures 1 and 5–8). This bone is straight in lateral view, a trait shared among pseudosuchians, and basal avemetatarsalians (i.e., aphanosaurs, silesaurids)
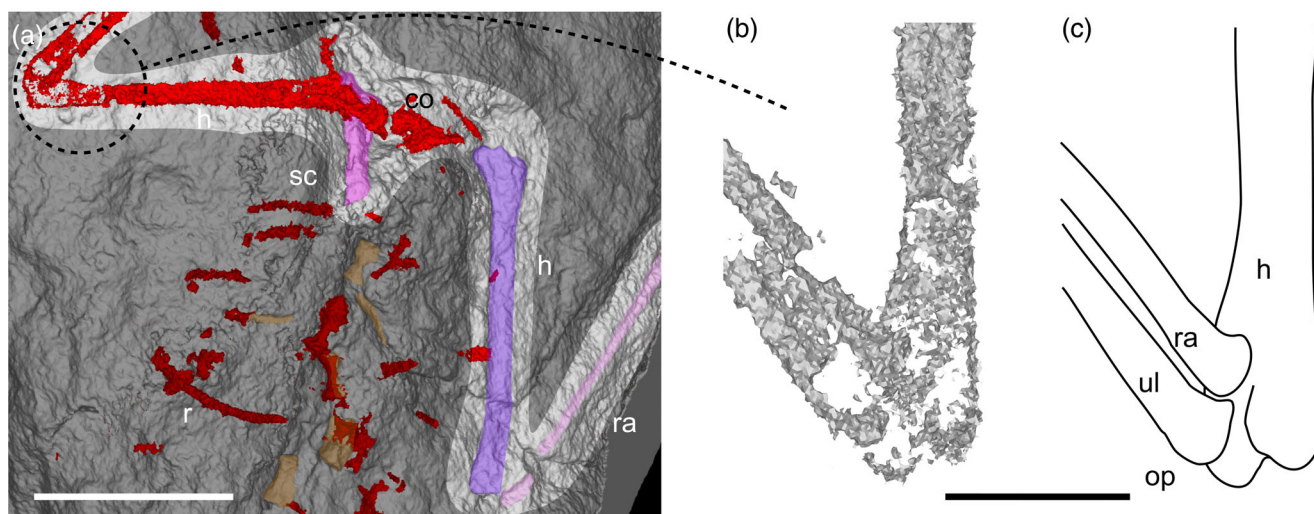
FIGURE 8 Elbow of *Scleromochlus taylori*. (a) Trunk and forelimbs of NHMUK PV R 3914 in ventral view. (b,c) Details of the elbow of the right arm in ventral view, and interpretative drawing. Scale bar equals 10 mm in a and 5 mm in b–c. See main text for abbreviations.

but not with pterosauromorphs (Ezcurra, Nesbitt, et al., 2020) and dinosaurs, whose humeri are distinctly sigmoidal in shape. *Scleromochlus* has a uniquely slender humerus with the lowest maximum proximal transverse width/total length ratio (~0.16–0.20) recorded in Archosauria (see tab. 2 in McCabe et al., 2021; Figures 5a and 6). The proximal end is medially expanded in anterior view and crescent-shaped in proximal view. The deltopectoral crest is short, reaching ~15%–18% of the total length of the bone, which is uniquely short within Pterosauromorpha, and perhaps only comparable to that of *Faxinalipterus minimus* (UFRGS-PV-0927-T). The crest has a subtriangular outline and is only weakly laterally expanded (Figures 5a and 6), as also occurs in *Faxinalipterus minimus* (UFRGS-PV-0927-T) and *Ixalerpeton polesinensis* (ULBRA-PVT059), in contrast to the strongly protruding crests present in pterosaurs (Cabreira et al., 2016; Ezcurra, Nesbitt, et al., 2020; Kellner et al., 2022; Padian, 1984). The distal end of the humerus is moderately expanded (contra Benton, 1999) as it is in *Lagerpeton chanarensis* (MCZ 101542; McCabe et al., 2021), and has a moderately large ectepicondyle (clearly visible in NHMUK PV R3556 and NHMUK PV R3914; Figures 5a, 6b–d, and 8), similar to those present in lagerpetids (i.e., *Ixalerpeton polesinensis*, ULBRA-PVT059; *Dromomeron romeri*, GR 238; *Faxinalipterus minimus*, UFRGS-PV-0927-T; Cabreira et al., 2016; Martz & Small, 2019; Kellner et al., 2022). The torsion between the distal and proximal end is narrow (estimated ~36°–38° in NHMUK PV R3556 and NHMUK PV R3557; Figure 6d,g), which is comparable to, but slightly higher than, that in other pterosauromorphs (see fig. 4 in Martz & Small, 2019).

Radius

Previous studies described the radius based on those preserved in NHMUK PV R3556, R3146, R5589, R4823/4, and the left radius of NHMUK PV R3914, but none of these bones are fully captured in the peels (Figure 2). In our scan data, however, the radii in NHMUK PV R3557 and NHMUK PV R3914 are now fully accessible digitally (Figure 7b,c). Combining all the available information, the radius of *Scleromochlus* is a straight bone that is nearly as long as the humerus (~92%–95% of its length) (Figures 2, 6a,e, 7c, and 8). The relative length of this bone was sometimes overestimated, presumably due to misinterpretations regarding the portions of forelimb elements preserved. For instance, von Huene (1914) and Bennett (2020) reported the radius of one individual, NHMUK PV R3146, to be equal in length to the humerus, but neither ends of the humerus or the radius are preserved sufficiently to support this claim. A similar misunderstanding could have risen when examining NHMUK PV R3556. As neither the radii nor the humeri are completely visible in the peels any measurement derived from this specimen must be an estimate. According to our data, the relative length of the radius to the humerus in *Scleromochlus* is greater than in basal dinosauromorphs (e.g., *Lagosuchus* ~0.64) and *Dromomeron romeri* (~0.78), but shorter than in *Silesaurus opolensis* (~1.00) and pterosaurs, which have a radius that is equal to or longer than the humerus (Dalla Vecchia, 2013; Dzik, 2003; Padian, 1984).

The forearm (radius and ulna) of *Scleromochlus taylori*, is considerably more slender (i.e., higher length-to-width ratio) than that of *Venetoraptor gassenae* (Müller et al., 2023).

Ulna

The ulna is also nearly as long as the humerus. Again, only partial surfaces are visible in the peels, but a complete ulna is present in NHMUK PV R3914 and now visible in the μCT scans. This is particularly useful as it reveals previously unknown features of its proximal end. Specifically, a low, triangular and poorly developed olecranon process is present (Figures 7c and 8). This contrasts with the ulna of *Venetoraptor gassenae*, which has a strongly developed olecranon process (Müller et al., 2023). Unfortunately, it is not possible to compare these features with those of other lagerpetids directly, as the latter taxa all lack complete ulnae. However, it is worth noting that early avemetatarsalians (e.g., *Teleocrater rhadinus*; Nesbitt et al., 2017), silesaurids and early pterosaurs also have a prominent but low olecranon (Dalla Vecchia, 2013; Wellnhofer, 2003; Wild, 1984). NHMUK PV R3914 also shows that the distal end of the ulna is rounded, and its distal surface is convex. In all these features, the ulna of *Scleromochlus* is remarkably similar to those of aphanosaurs and *Silesaurus opolensis* (Dzik, 2003). Because *Scleromochlus taylori* shares these features with aphanosaurs and silesaurids, but also some early pterosaurs (Dalla Vecchia, 2013; Dzik, 2003; Nesbitt et al., 2017, 2020), it is possible that they are symplesiomorphies of early pterosauromorphs.

Manus

Benton (1999) described fragmentary hands in NHMUK PV R3556 and NHMUK PV R4823/4. Further details of the manus are revealed by the μCT scan data from NHMUK PV R3914, NHMUK PV R4823/4, and NHMUK PV R3557 (Figure 7). These specimens show that the manus of *Scleromochlus taylori* is not modified for flying (e.g., by possessing anything resembling the elongate fourth digit of pterosaurs) and that it is not dissimilar to those of other basal avemetatarsalians. The manus might have ossified carpals, but their presence is hard to confirm due to their size and the scan resolution (Figure 7). We concur with Benton (1999) that the manus is short, compared with both the forelimb and hindlimb. The longest digit (including the metacarpal) is likely much shorter than the humerus, and the longest metacarpal (II–IV) is only ~18% the length of the longest metatarsals, and less than 10% of humeral (and radius/ulna) length. By contrast, in Pterosauria and *Dromomeron romeri* (GR238: the only lagerpetid for which this state can be scored), metacarpal III is equal to or longer than 35% of humeral length. This state cannot be assessed for *Venetoraptor gassenae* because the humerus of this taxon is missing. However, digit III of *Venetoraptor gassenae* (and *Dromomeron romeri* and *Ixalerpeton polesinensis*)

(Müller et al., 2023) is longer than the radius/ulna length, while the opposite (i.e., digit III considerably shorter than radius/ulna length) is true in *Scleromochlus taylori*. Altogether these data suggest that a comparatively short manus could be unique for *Scleromochlus* within Pterosauromorpha, or that a longer manus was independently acquired in Pterosauria and Lagerpetidae (Müller et al., 2023). All the metacarpals of NHMUK PV R3914 and NHMUK PV R4823/4 are elongate (e.g., the first metacarpal is roughly five times longer than wide at its distal end), have partially overlapping proximal ends, are symmetrical, and lack extensor pits at their distal ends. Expanded, or particularly deep, distal ends are not seen in any other specimen with metacarpals. It is however possible that these structures are too small to be observed with the resolution of available scans. The metacarpals are subequal in length, and the shortest (metacarpal I) is only slightly shorter and thicker than the longest (metacarpals II–IV). Notable is the presence of a metacarpal V, whose presence is unclear in *Teleocrater rhadinus* (Nesbitt et al., 2017), but it is present and associated with a single vestigial phalanx in *Venetoraptor gassenae* (Müller et al., 2023), is reduced to a splint-like element in *Dromomeron romeri* (Ezcurra, Nesbitt, et al., 2020), and is absent altogether in pterosaurs (Dalla Vecchia, 2013). It is unknown, however, if there are distal phalanges associated with metacarpal V in *Scleromochlus*.

Manual phalanges are present in NHMUK PV R3557, NHMUK PV R3914, and NUMUK PV R4823/4, and are shorter than the metacarpals (Figure 7). Due to the size and preservation of the distal phalanges, it is hard to determine the phalangeal formula, and none of the manual unguals are sufficiently well preserved to be described. *Scleromochlus* does not possess enlarged trenchant claws like those of *Venetoraptor gassenae* (Müller et al., 2023). The hand of *Scleromochlus* also lacks either an elongated digit IV or a pteroid, both of which are features that are diagnostic of Pterosauria.

4.1.7 | Pelvic girdle and hindlimbs

As exposed in NHMUK PV R3556 and NHMUK PV R3557, the acetabulum faces mainly laterally. The ilium of *Scleromochlus* is similar to those of other lagerpetids, in that it is small (shorter than twice the acetabular height) and its dorsal margin is concave, with a concavity level or slightly posteriorly displaced from the acetabulum (Sereno & Arcucci, 1994). The ilium has a distinct preacetabular process (but not as well developed as those in pterosaurs) and an anteroposteriorly expanded pubic peduncle (Figure 9; Arcucci, 1986; Cabreira et al., 2016; Ezcurra, Nesbitt, et al., 2020). As in *Ixalerpeton* and
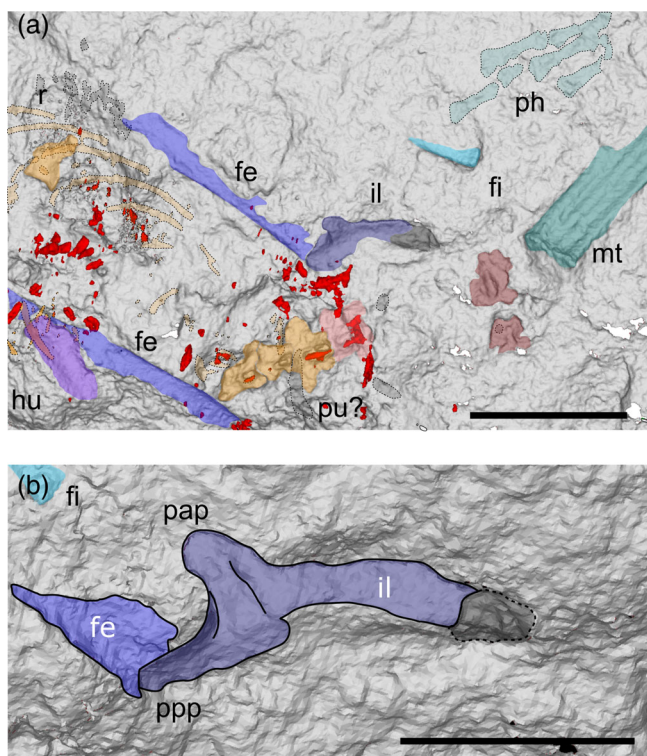
FIGURE 9 Pelvic girdle of *Scleromochlus taylori*. (a) dorsal slab of NHMUK PV R3557 in dorsal view. (b) detail of the left ilium in lateral view. Scale bar equals 10 mm. See main text for abbreviations.

Lagerpeton, the ilium of *Scleromochlus* bears a lateral crest that is confluent with the preacetabular process (Figure 9; Arcucci, 1986; Cabreira et al., 2016; Ezcurra, Nesbitt, et al., 2020).

It is unlikely that the peels of NHMUK PV R3556 and NHMUK PV R3557 captured the full extent of the ischium and pubis ventrally due to the fragility of these bones. Their orientations as described by previous authors (Bennett, 2020; Benton, 1999) are likely accurate, with the pubic shaft oriented in an anteroventral direction and the ischium directed posteroventrally (see fig. 13b in Benton, 1999). As in aphanosaurs, silesaurids and most lagerpetids (Dzik, 2003; Nesbitt et al., 2017; Yáñez et al., 2021), the pelvic girdle is not reinforced and lacks enlarged muscle attachments, contrasting with the presence of these features in pterosaurs (Hyder et al., 2014).

Femur

The μCT scan data reveal numerous key details of the femur in *Scleromochlus* that were unavailable in the peels or through inspection of the original specimens. This new information comes from femora enclosed within the sandstone matrix of NHMUK PV R4823/4 and NHMUK PV R3146. Overall, the femur of *Scleromochlus* is elongate, weakly sigmoid, and ~145%–155% of the total

length of the humerus, and with a minimum width that is ~147%–160% that of the humerus. The femur has gracile proportions (ratio of distal transverse width to total length, ~0.11), much lower than that of other lagerpetids (e.g., in *Ixalerpeton*, *Lagerpeton, Dromomeron romeri* and *D. gregorii* these values are closer to ~0.15–0.20), and most other Triassic archosaurs (Figures 10 and 11; e.g., ~0.16 in *Silesaurus opolensis* [ZPAL AbIII/361/25]; ~0.14 in *Dimorphodon*; up to higher values in many pseudosuchians: e.g., ~0.27 in *Aetosauroides scagliai* [PVL 2073]; 0.33 in *Riojasuchus tenuisceps* [PVL 3827]; Ezcurra, 2016). The proximal head is roughly oval in distal view and its long axis forms an acute angle (~30°) with the line though the femoral condyles in proximal/distal view (Figure 10l). The articular surface is in-turned medially, a feature that gives the proximal femur a distinctive hook-shaped aspect, which also is present in lagerpetids and early pterosaurs, and diagnostic of Pterosauromorpha (Ezcurra, Nesbitt, et al., 2020). The transition between the shaft and the femoral head is a concave emargination that *Scleromochlus* shares with lagerpetids and pterosaurs (Figure 10g–i; Ezcurra, Nesbitt, et al., 2020).

New data from the femur in NHMUK PV R4823/4 are particularly helpful in elucidating the presence and shapes of the muscle attachments on the medial side of the shaft (Figure 11). Based on this specimen, *Scleromochlus* has a low fourth trochanter that has symmetrical proximal and distal margins—this feature is also visible in the left femur of the type specimen (NHMUK PV R3556; Figures 10a,b and 11) (*contra* Sereno, 1991). The presence of a fourth trochanter in *Scleromochlus* has been debated, and its supposed absence was used to support a close relationship between this taxon and pterosaurs (Ezcurra, Nesbitt, et al., 2020; Sereno, 1991). However, this feature is variably present in pterosauromorphs (Ezcurra, Nesbitt, et al., 2020; Kammerer et al., 2020) and the morphology of this structure is strongly plastic through ontogeny (Griffin et al., 2019). Based on our observations, the fourth trochanter of *Scleromochlus* extends across the proximal quarter of the femoral length and separated from the femoral head, as also seen in *Dromomeron gregori*, but in contrast to *Lagerpeton chanarensis* (Nesbitt et al., 2009), where it is longer and extends across the proximal third of the femur. The attachment for the M. caudofemoralis in *Scleromochlus* is a low rugose ridge/scar, as in *Dromomeron romeri* (GR 218) and *D. gigas* (PVSJ 898), but in contrast to those of *D. gregori* (TMM 31100–1306), *Lagerpeton chanarensis* (PULR 06; PVL 4619), *Kongonaphon kely* (UA 10618), and *Ixalerpeton polesinensis* (ULBRA-PVT059), which each have a distinct, sharp, crest-like attachment point (Cabreira et al., 2016; Ezcurra, Nesbitt, et al., 2020;
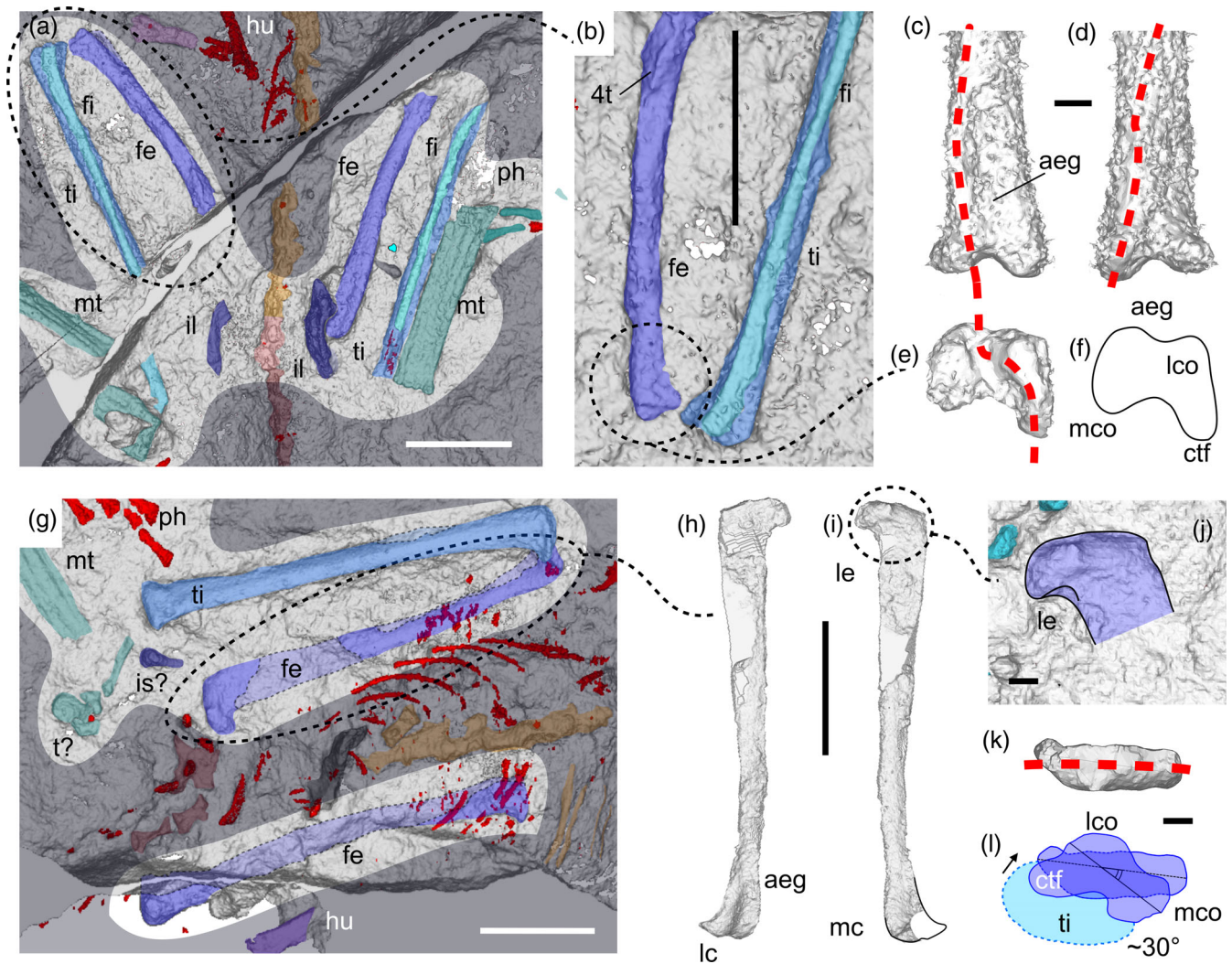
FIGURE 10 Femur and hindlimb of *Scleromochlus taylori*. (a) NHMUK PV R3556, hindlimbs and pelvic girdle in dorsal view. (b) Details of the left femur (rotated in medial view), tibia and fibula. (c–f) Details of the distal end of the left femur in anterior (c), posterior (d), distal (e,f) views. (g) NHMUK PV R3557, proximal hindlimb elements in ventral view. (h,i) Close-ups of the right femur in anterior (h) and medial (i) views. (j,k) Details and interpretative drawings of the right femur: close-up of the femoral head in medial (j) and proximal (k) views. (l) interpretative drawings showing the relative orientation of the femoral head (dark) and distal end (light). Digital rendering of the peels in grey; previously unavailable details are figured in bright red. Scale bars equal 10 mm in a, b, g, h and 1 mm in c–f, j–l. See main text for abbreviations.

Griffin et al., 2019; Irmis et al., 2007; Kammerer et al., 2020; Nesbitt et al., 2009).

The distal end of the femur bears two prominent condyles (Figure 10e,f,l). These are separated by a shallow extensor groove on the anterior surface of the femur. These features are visible in all specimens, and their presence is further confirmed in the newly segmented femora of both of the individuals in NHMUK PV R3146 (Figures 2 and 11h–m). *Scleromochlus* shares with lagerpetids the presence of a prominent crista tibiofibularis (Ezcurra, Nesbitt, et al., 2020), which is particularly clear in the μCT scans of NHMUK PV R3556, NHMUK PV R3557, and NHMUK PV R3146 (Figures 10e–f,l and

11h–m). Note that the crista tibiofibularis was misidentified as the lateral condyle in NHMUK PV R3557 by Bennett (2020). Due to the poor preservation of most Triassic pterosaurs, it is not clear whether an enlarged crista tibiofibularis is an autapomorphy of Pterosauromorpha or only of Lagerpetidae.

Tibia

The tibia and fibula are both longer than the femur, even more so than previously reported. As in other lagerpetids (Cabreira et al., 2016; Nesbitt et al., 2017), the tibia is ~109%–118% the length of the femur, against 104% estimated by Benton (1999), but it is still comparatively
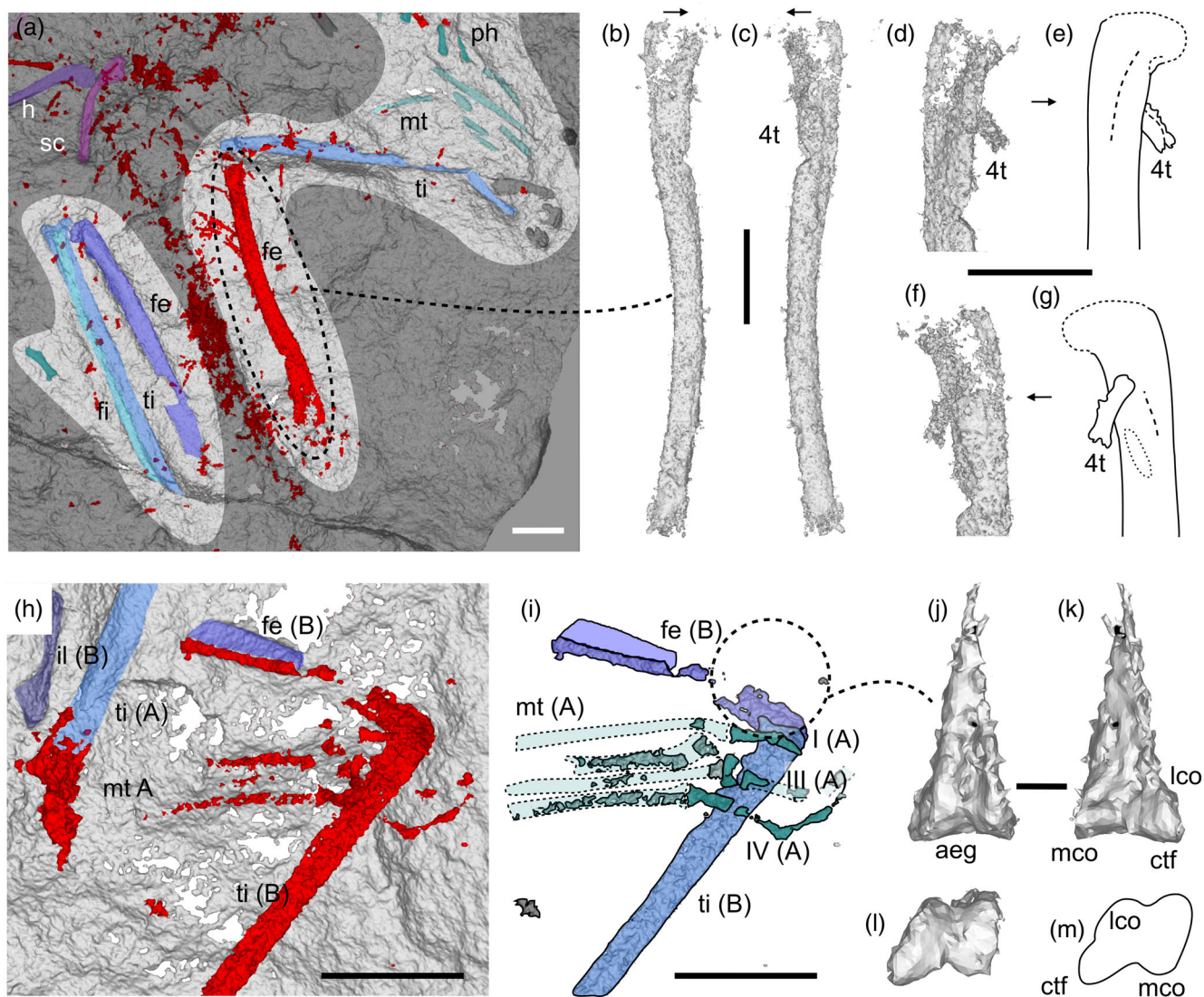
FIGURE 11 Femur and hindlimb of *Scleromochlus taylori*. (a) NHMUK PV R4823/4, skeleton in dorsal view. (b–g) NHMUK PV R4823/4 right femur in lateral (b), medial (c) views; close-up and line drawings of the femoral head in lateral (d, e) and medial (f, g) views. (h–m) NHMUK PV R3146, details of the right knee and in dorsal view (h, i), and distal end of the femur in anterior (j), posterior (k), and distal views (l, m). Scale bars equal 10 mm in a–i, 1 mm in j–m. See main text for abbreviations.

shorter than those of pterosaurs (except perhaps *Peteinosaurus zambellii*; Wild, 1978; Jenkins et al., 2001; Dalla Vecchia, 2013, 2019). The μCT scan data allowed better visualization of the proximal tibia in several specimens (NHMUK PV R3556 and R3557; Figures 2 and 10a,b,g). The tibia has a distinct, anteriorly straight cnemial crest, a feature that lagerpetids share with some basal ornithodirans (i.e., *Silesaurus opolensis*, *Asilisaurus kongwe*, *Lagosuchus talampayensis*; Dzik, 2003; Nesbitt et al., 2010; Angolin & Ezcurra, 2019). The lateral side of the tibia is unknown because it is covered by the closely appressed fibula in all specimens (Figures 2, 10a,b,g, and 11a). The distal end of the right tibia of NHMUK PV R3146 (in the smallest individual, B) is visible in the μCT

scans and its lateral side is smooth and rounded (perhaps weakly concave) and lacks any obvious grooves or slots for articulations with the ankle bones. The tibia and fibula are not fused.

Fibula

The fibula of *Scleromochlus* is a slender, straight element that is subequal in length to the tibia, but markedly thinner (Figures 2, 10a,b,g, and 11a; Bennett, 2020; Benton, 1999; von Huene, 1914; Woodward, 1907). This morphology is seen clearly in NHMUK PV R3556, NHMUK PV R3914, and NHMUK PV R3146. The fibula has a transversely compressed proximal head that is slightly asymmetrical and expands posteriorly, as in most

ornithodirans. The anterior margin of the shaft is rounded in NHMUK PV R3556, similar to that of *Lagerpeton chanarensis*, *Dromomeron romeri*, and *Lagosuchus talampayensis*, but unlike that of most other ornithodirans, in which the anterior margin tapers to a point.

The attachment site for the M. iliofibularis lies entirely on the proximal quarter of the bone, close to the proximal head (NHMUK PV R3556; Figure 10a,b). The distal end of the fibula is rounded (NHMUK PV R3146 and NHMUK PV R3914), similar to the condition in *Lagerpeton chanarensis* and *Ixalerpeton polesinensis* but unlike some pterosaurs (*Peteinosaurus zambellii* and *Dimorphodon macronyx*).

Note that the fibula of NHMUK PV R3557 was previously misidentified in the casts, resulting in inconsistencies in the description of this element. The bone previously identified as the right fibula in NHMUK PV R3557 (Benton, 1999) is likely a left humerus, which is disarticulated from the pectoral girdle (Figure 5b). The left fibula of this specimen is still articulated with the tibia, as shown by the incomplete proximal end of this bone, which lies behind the medial side of the left tibia.

Astragalus, calcaneum, and tarsals

The interpretation of the astragalus, calcaneum, and tarsals has the subject of considerable debate. Unfortunately, we could not identify each element with confidence, even using the μCT scans. We recommend that the ankle scores are left as "?" in phylogenetic analyses (Foffa et al., 2022). Importantly, we earlier showed that different interpretations of the ankles do not affect the results of phylogenetic analyses (Foffa et al., 2022). For more information, we refer to the extensive discussion in Foffa et al. (2022).

Pes and unguals

Scleromochlus has five metatarsals. They are not capped by distal tarsals, which are, in our opinion, absent (Foffa et al., 2022), in contrast to previous reports (Benton, 1999; Bennett, 2020). Metatarsals I–IV are subequal in length and closely appressed (Figures 2, 5, and 9–13; Bennett, 2020; Benton, 1999; Padian, 1984; von Huene, 1914; Woodward, 1907). As this condition occurs in all six specimens, we consider it unlikely to be a preservational artefact. The metatarsals are between 50% and 57% the length of the tibia (45%–47% estimated by Benton, 1999). Metatarsal I is unusually long and only slightly shorter than metatarsals II–IV (Figures 9–13). This is a feature that *Scleromochlus* shares with pterosaurs, which distinguishes it from *Lagerpeton chanarensis*, *Dromomeron* spp., silesaurids, and basal dinosauromorphs (Dzik, 2003; Romer, 1971a; Sereno &

Arcucci, 1994). Metatarsal IV measures 50%–59% of the length of the tibia, and is straight, as in pterosaurs, rather than laterally curved at its distal end as in *Lagerpeton chanarensis* (PULR 06; PVL 4619). Metatarsal V is articulated with the remainder of the foot only in NHMUK PV R3556, although it is closely associated with the remainder of the metatarsus in NHMUK PV R5589. We concur with Sereno (1991), Benton (1999), and Bennett (2020) in their interpretations of the right metatarsal V of NHMUK PV R3557. Based on our observations we confirm that metatarsal V is shorter than 50% of the length of metatarsal III, as in other pterosauromorphs. No distal phalanges are seen with metatarsal V in any specimen. The absence of distal phalanges associated with metatarsal V also occurs in *Lagerpeton chanarensis* (Romer, 1971b) but not in pterosaurs (Hone et al., 2012). Note that due to excessive mechanical alteration of the specimen, metatarsal V can no longer be identified with confidence in NHMUK PV R3556.

Before obtaining our μCT scan data, all that was known of the foot of *Scleromochlus taylori* were partial surfaces and isolated impressions of individual phalanges. The best-preserved feet in the peels are those of NHMUK PV R3556, which are visible as a partial impression on both slabs (Figures 2 and 13a). This specimen shows that the foot (longest articulated metatarsal and digit) of *Scleromochlus* is slightly longer than the tibia, as in *Lagerpeton chanarensis* (PVL 4619) and *Dromomeron romeri* (SP NUMBER) (the only lagerpetids for which such data are available), but unlike the condition in pterosaurs, where the foot is comparatively shorter. The impressions of partial phalanges, which are rarely articulated, can be seen in other specimens, but not particularly informative. Based on these data, Benton (1999) suggested a phalangeal formula of ?-?-4-5-0.

Additional data are now available from μCT scans of NHMUK PV R3556, NHMUK PV R3557, and NHMUK PV R3914. The latter preserves a nearly complete foot. Pedal digit IV is less well-preserved than the others, but when information from all of the specimens is combined the foot of *Scleromochlus* is now completely known (Figure 12). These data allow us to confidently amend the pedal phalangeal formula to 2-3-4-5-0. None of the specimens possesses a phalanx or ungual associated with pedal digit V. The pedal phalangeal formula of *Scleromochlus taylori* is the same as in *Lagerpeton chanarensis* (PVL 4619; Sereno & Arcucci, 1994) and basal dinosauromorphs (Nesbitt, 2011), while it is typically 2-3-4-5-2 in non-pterodactyloid pterosaurs (Hone et al., 2012).

A striking feature of the foot of *Scleromochlus* is the elongation of the phalanges. NHMUK PV R3556, NHMUK PV R3557, NHMUK PV R3914, and NHMUK PV R5589 show that all the preserved phalanges are
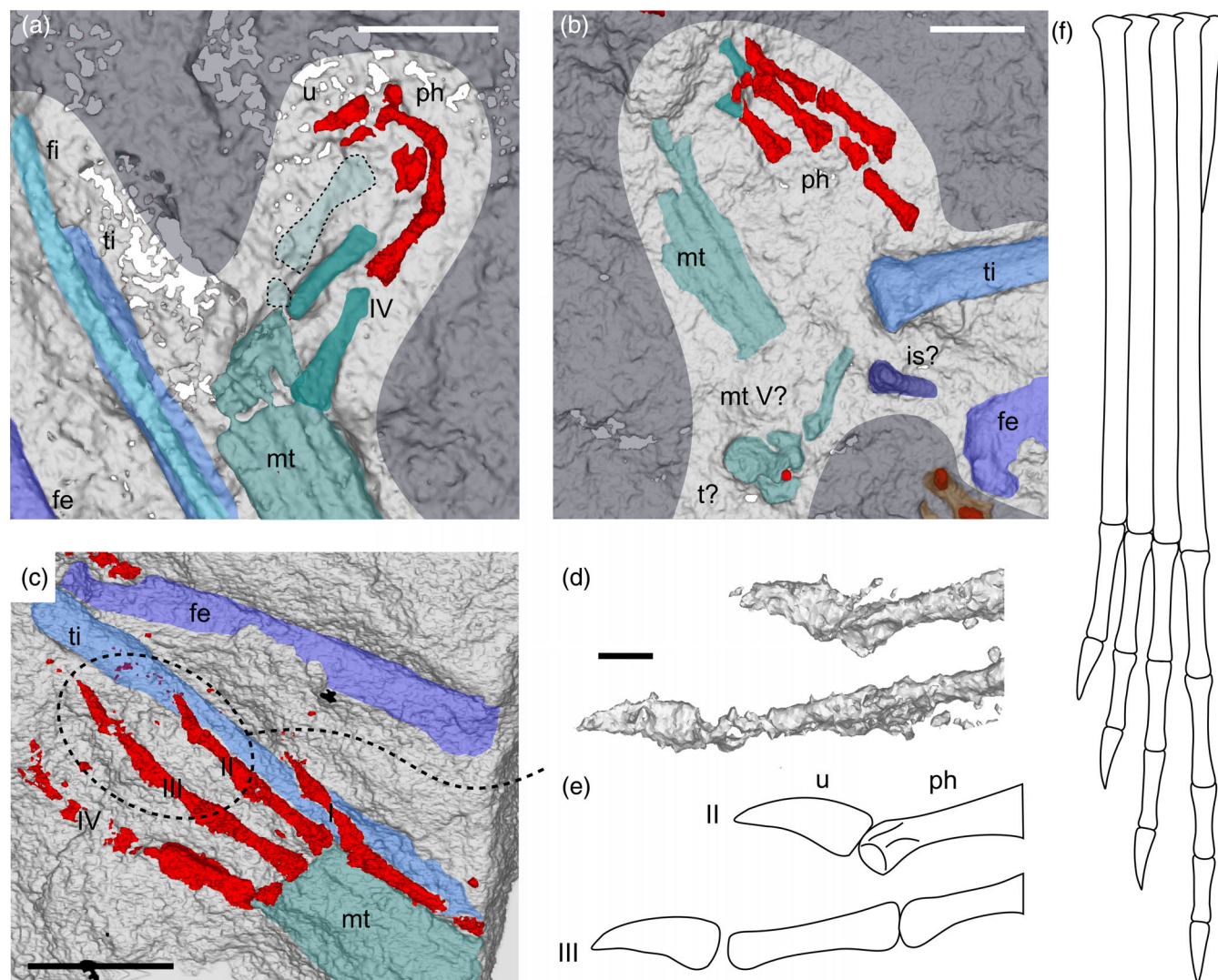
FIGURE 12 Pes of *Scleromochlus taylori*. (a) NHMUK PV R3556, close-up of the right pes (metatarsals, complete digit IV and phalanges) on the dorsal slab. (b) NHMUK PV R3557, metatarsals and phalanges of the right pes. (c) NHMUK PV R3914, complete right pes in ventral view. (d,e) NHMUK PV R3914, details and line drawings of the terminal phalanges and ungual of digit II and III in medial view. (f) Schematic reconstruction of the complete pes of *Scleromochlus taylori* based on all available specimens. Scale bars equal 5 mm in a–c, 1 mm in d, e and 10 mm in f. See main text for abbreviations.

subequal in length and have high length/width ratios, as opposed to those in some basal pterosaurs where the proximal phalanges are longer than the distal ones (Figure 12). Similar to *Lagerpeton chanarensis* (PVL 4619), digit IV of *Scleromochlus* is the longest, followed by III, II, and I, with digit III slightly angled relative to the midline (Sereno & Arcucci, 1994). However, even if digits I and II of *Scleromochlus taylori* are comparatively long their metatarsal–phalangeal joints are roughly in line with those of the other digits (Figure 12). In these features, the pes of *Scleromochlus taylori* more closely corresponds to the features of the Early–Middle Triassic ichnogenus *Prorotodactylus*, than does the foot of *Lagerpeton chanarensis*, which some studies have argued shares key synapomorphies with the *Prorotodactylus*

footprints (Brusatte et al., 2011; Niedźwiedzki et al., 2013), We note that the potential track maker of *Prorotodactylus* may also be a different type of basal ave-metatarsalian (Fitcher & Kunz, 2013; Mujal et al., 2017; Padian, 2012). Regardless of the affinities of *Prorotodactylus*, a *Sclerlomochlus* type-foot might be plesiomorphic for Pterosauromorpha, suggesting that the "functionally didactyl" condition in *Lagerpeton chanarensis* (and likely other lagerpetids) is a derived condition with respect to other avemetatarsalians.

The unguals of digits II–III–IV in NHMUK PV R3914 are well preserved (Figure 12c–e). They have triangular cross-sections, are weakly transversely compressed, and lack conspicuous ventral tubercles, which contrast with well-developed tubercles present in most basal
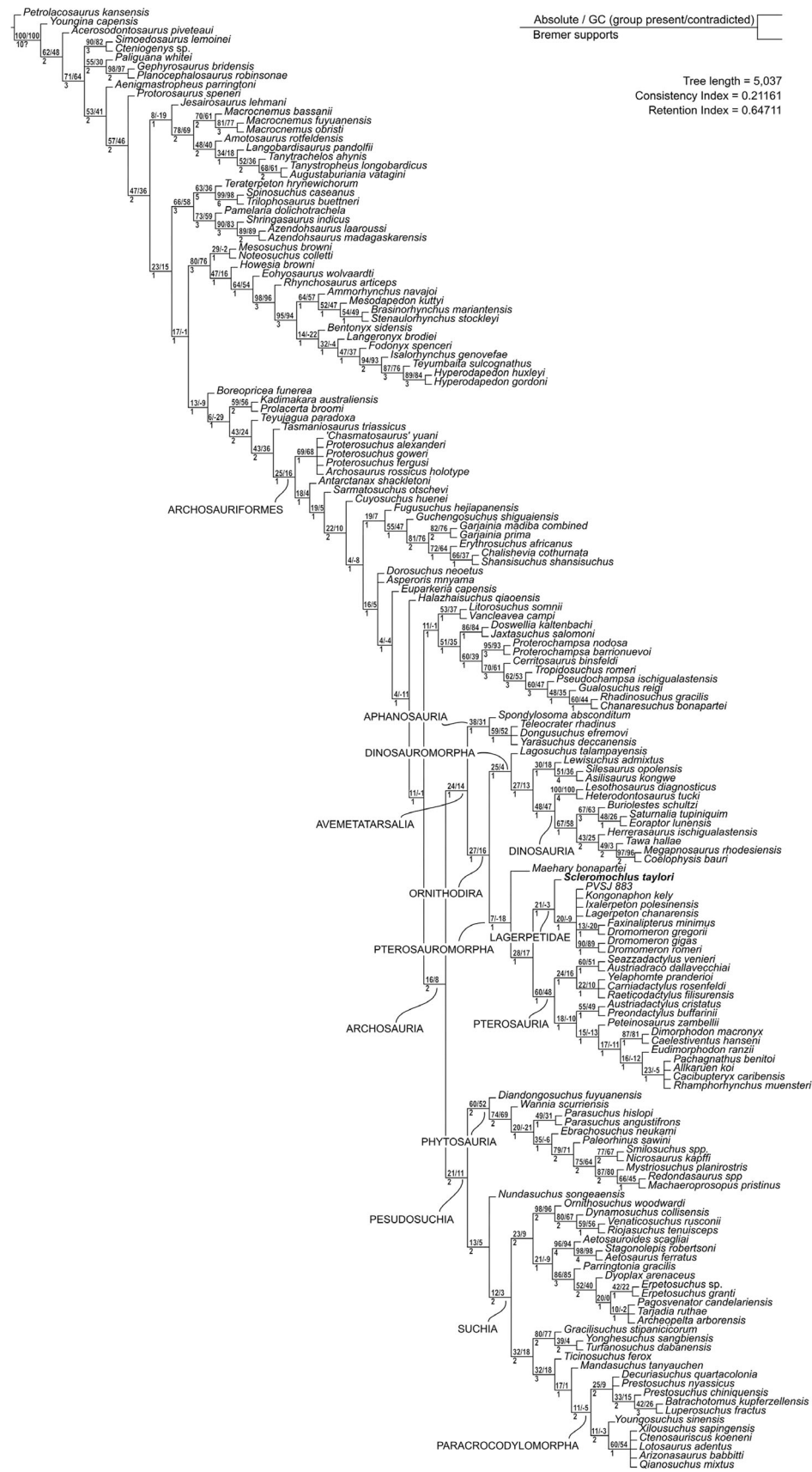
Absolute / GC (group present/contradicted)
Bremer supports

Tree length = 5,037
Consistency Index = 0.21161
Retention Index = 0.64711

FIGURE 13 Strict consensus trees of the maximum parsimony analysis.

pterosaurs. Other pedal unguals are visible in less detail in NHMUK PV R3556 and NHMUK PV R5589 but help to confirm that the pedal unguals are shorter than the corresponding penultimate phalanges.

Unidentified structures

It has been suggested that osteoderms covered the posterior dorsal area of at least three *Scleromochlus* specimens (NHMUK PV R53557, NHMUK PV R3146, and NHMUK PV R4823/4; Bennett, 2020; Benton, 1999; Padian, 1984; von Huene, 1914; Woodward, 1907). These putative structures are faintly visible in the peels and original specimens, but they are not apparent in the μCT scans, nor are there any other structures within the matrix that could represent osteoderms. Consequently, we reject the presence of osteoderms in *Scleromochlus* (contra Bennett, 2020; Benton, 1999; von Huene, 1914; Woodward, 1907). It is worth noting that a cluster of long, curved elements is present in NHMUK PV R3557, where they are misaligned on the dorsal side of the mid-dorsal area, and in NHMUK PV R4823/4, where they occur among disarticulated elements of the anterior trunk. These elements are circular in cross-section but are unlikely to be ribs, as they are wider in diameter and do not articulate with the vertebrae. Both their extremities are concave, and it is unclear whether they belong together with the skeletons. Due to their position, size and shape we consider it unlikely that they represent osteoderms.

Finally, an elongate structure is present in the pelvic region of the largest individual of NHMUK PV R3146. It is conceivable that it represents an egg or a coprolite, but it might be a nodule or another geological feature (Figure 2).

4.2 | Phylogenetic analyses

The taxon-character matrix we analyze here is identical to that of Foffa et al. (2022), with the exceptions of the inclusions of the purported pterosauromorphs *Maehary bonapartei*, *Faxinalipterus minimus*, and the newly described pterosaurs *Pachagnathus benitoi* and *Yelaphomte praderioi*. Unsurprisingly, the relationships between the major groups and the position of *Scleromochlus* are maintained, and thus the overall tree topology will not be discussed further. Instead, we focus on the effects of including these new taxa compared with the results of Foffa et al. (2022).

4.2.1 | Maximum parsimony analyses

We recovered 1560 MPTs with lengths of 5037 steps, with CI = 0.21161 and RI = 0.64711, compared with the

880 MPTs of 5021 steps with CI = 0.21207 and RI = 0.64693 from the earlier analysis of Foffa et al. (2022).

Scleromochlus taylori is still found in Pterosauromorpha as the earliest-diverging lagerpetid. Consistent with the results of Kellner et al. (2022), *Maehary bonapartei* is found as the earliest diverging pterosauromorph (i.e., sister taxon to a clade formed by Lagerpetidae + Pterosauria). *Faxinalipterus minimus* is recovered nested within Lagerpetidae, as the sister taxon of *Dromomeron gregorii* (supported only by the presence of an anterior offset of the lateral posterior condyle of the tibia from the medial condyle), implying polyphyly of *Dromomeron*. *Yelaphomte pradeiroi* and *Pachagnathus benitoi* are found in positions consistent with those found by Martínez et al. (2022), in their analysis based on the Ezcurra, Nesbitt, et al. (2020) dataset: *Yelaphomte* is recovered in Pterosauria, in a polytomy with *Carniadactylus* and *Raeticodactylus* in a clade that also contains *Sezzadactylus* and *Austriadraco*; *Pachagnathus* is also recovered in Pterosauria, in a polytomy with *Allkauren*, *Cacibupteryx*, and *Rhamphorhynchus*. Note, however, that Martínez et al. (2022) considered both *Yelaphomte* and *Pachagnathus* as raeticodactylids following the results of their pterosaur-only analysis.

Forcing *Scleromochlus taylori* to become the earliest-branching taxon in Pterosauromorpha (Ezcurra, Nesbitt, et al., 2020) produces slightly shorter MPTs than constraining it as sister taxon to Pterosauria (Gauthier, 1984, 1986; Padian, 1984; Sereno, 1991). These options require two and three additional steps, respectively, compared with the MPTs.

Enforcing any other historical phylogenetic hypotheses produces substantially less parsimonious trees than those obtained in an unconstrained analysis. Forcing *Scleromochlus* to be the sister taxon of (Dinosauriformes: i.e., *Lagosuchus talampayensis* + Dracohors) (Bennett, 1996) and at the base of Ornithodira (Benton, 1999) requires 37 additional steps; constraining *Scleromochlus taylori* to the base of Avemetatarsalia requires 133 additional steps; placing *Scleromochlus taylori* in Doswellidae (Bennett, 2020) requires 22 additional steps; removing *Scleromochlus taylori* from Archosauria requires 213 additional steps; and forcing *Scleromochlus taylori* to the base of Archosauriformes (Bennett, 2020) requires over 230 additional steps (Table 2).

4.2.2 | Bayesian inference analysis

The unconstrained Bayesian analyses produced a consensus tree that differs in topology from the strict consensus of the MPTs from the maximum parsimony analysis. Specifically, *Maehary* is not recovered in Pterosauromorpha

TABLE 2 Support for historical hypotheses of phylogenetic relationships of *Scleromochlus taylori* compared with our MPTs.

	MPTs score	+steps
Hypothesis		
Scleromochlus + Pterosauria	5039	2
Scleromochlus + Pterosauromorpha	5040	3
Sister taxon to Dinosauromorpha	5074	37
Basal avemetatarsalian (non-aphanosaurian and non-pterosaur avemetatarsalian)	5170	133
In Doswellidae	5059	22
In Pseudosuchia	5086	49
In Ornithosuchidae	5072	35
Basal archosauromorph	5267	230

but in Dinosauromorpha, as the sister taxon to Dinosauria, in a clade that forms a polytomy with Silesauridae and *Lewisuchus* (Figure 14). In Lagerpetidae, *Scleromochlus* is found as the earliest-branching taxon, and the monophyly of *Dromomeron* is maintained in a clade that includes PVSJ 883 as its earliest-branching member, and that grouping forms a polytomy with *Faxinalipterus*, *Lagerpeton*, *Ixalerpeton*, and *Kongonaphon*.

5 | DISCUSSION

This study highlights the limitations of traditional study techniques (i.e., molds, peels, casts) in previous attempts to understand the osteology of *Scleromochlus* (Foffa et al., 2022), and probably by extension, other similarly preserved taxa (Foffa et al., 2020). Finer details of the extremities of the long bones, limbs, ribs, tail, and cranium were particularly affected by this issue, which were all poorly known or misunderstood before this work. μCT scanning techniques resolve some of these issues. Digital reconstructions make it easier to assess the full extent of taphonomic deformation, allow easier and more objective interpretations of the known portions of the skeletons, and enable more complete visualizations and measurements of individual bones, particularly those that are split between two slabs or are only partially visible.

From a phylogenetic point of view, the new anatomical information gained from the μCT scan data have had the overall effect of stabilizing the position of *Scleromochlus taylori* within Archosauria, Avemetatarsalia, Ornithodira, Pterosauromorpha, and Lagerpetidae. We can also explore the reduced support for some historical hypotheses regarding the phylogenetic relationships of *Scleromochlus taylori* (see supp. inf. of Foffa et al., 2022).

Scleromochlus taylori lacks any of the current or historically proposed diagnostic features of any basal archosauriform clade (i.e., "Proterosuchia"; David et al., 1997; Ezcurra et al., 2013; Ezcurra, Jones, et al., 2020), doswellids (Sues et al., 2013), pseudosuchians (Broom, 1913; Charig, 1967; Kuhn, 1966; Romer, 1956; Romer, 1971a; von Huene, 1922; von Huene, 1942; Walker, 1970; Watson, 1917; Young, 1964) or dinosaurs (Romer, 1966; Swinton, 1970). The similarities between *Scleromochlus*, aphanosaurs, and basal dinosauromorphs are now regarded as avemetatarsalians plesiomorphies (see above). Below, we expand on the implications of these results in relation to modern and historical taxonomic definitions, using our maximum parsimony analysis as reference.

5.1 | Discussion of historical hypotheses

5.1.1 | *Scleromochlus taylori* outside Archosauria

In our analysis *Scleromochlus taylori* has two unambiguous diagnostic features of Archosauria (i.e., a medially expanded/asymmetrical proximal end of the humerus in anterior view; attachment of the iliofibularis muscle on a low distinct tubercle) and cannot be scored for seven others. Among the latter, we find it unlikely that this taxon possessed vomerine, palatine and/or pterygoid teeth, but an argument could be made for these to be too small to be detected. It is also unclear, but likely (see NHMUK PV R3556 and NHMUK PV R3557), that the antorbital fossa extended onto the horizontal (=posterior) process of the maxilla. In addition, *Scleromochlus* lacks several historical diagnostic features of other major basal archosauriform clades. For instance, the mid-dorsal vertebrae of *Scleromochlus* are unusually elongated rather than short as in Proterosuchidae and Erythrosuchidae ("Proterosuchia" in David et al., 1997; Ezcurra et al., 2013; Ezcurra, Jones, et al., 2020). Overall, removing *Scleromochlus* from Archosauria requires 213 (5250 steps) additional steps compared with the MPTs from our primary analysis.

5.1.2 | *Scleromochlus taylori* in Doswelliidae

Bennett (2020) hypothesized close relationships between *Scleromochlus* and doswelliids, a result that, as he noted, requires the losses of distal tarsals I and II, which Bennett (2020) considered absent in *Scleromochlus*. We agree on the absence of distal tarsals I–IV (Foffa et al., 2022), but noted that the systematics and taxonomy of Doswelliidae as used in Bennett's (2020) analysis has since become
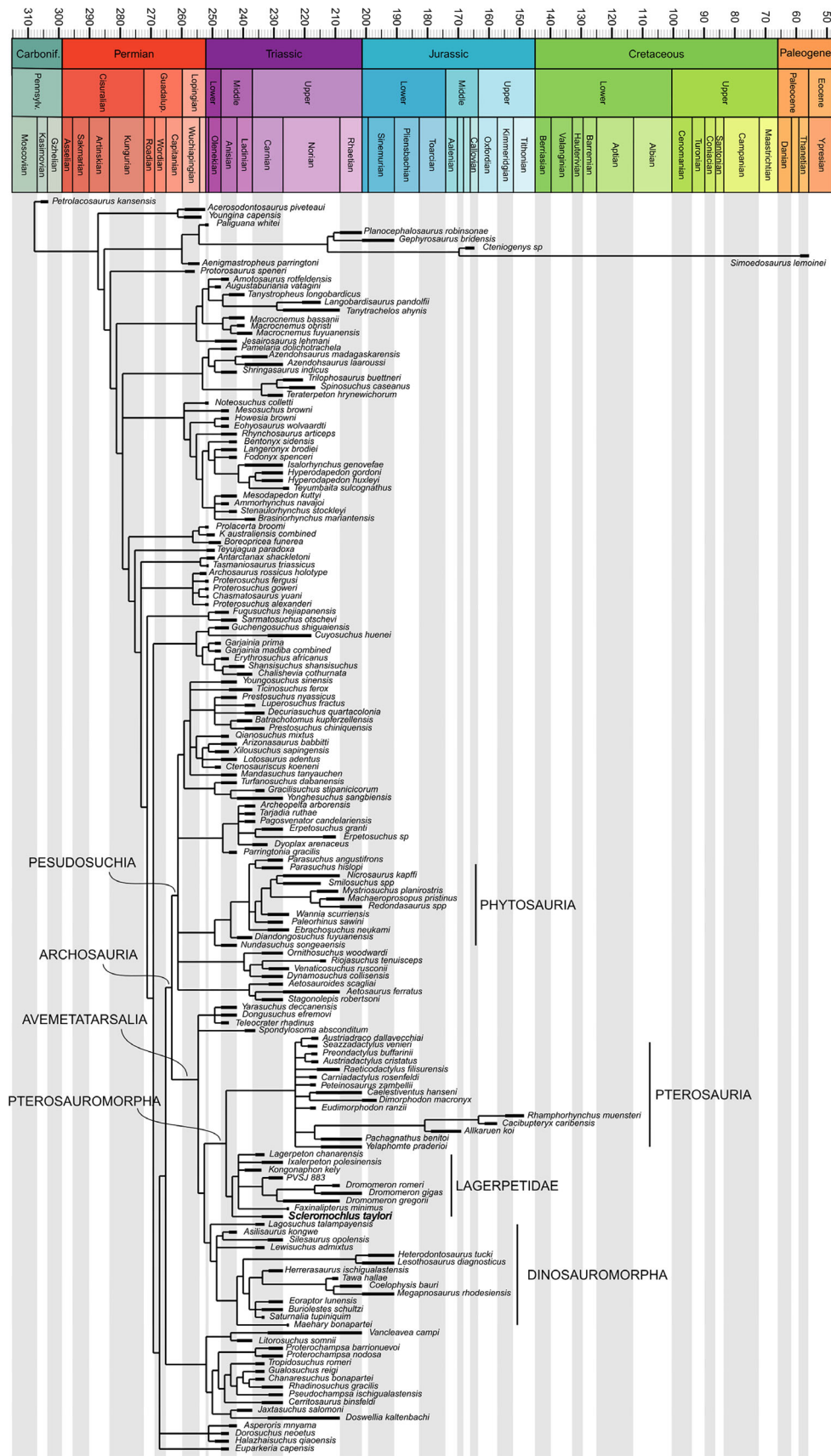
FIGURE 14 Consensus of the Bayesian Inference phylogenetic analyses.

outdated (i.e., *Tarjadia ruthae* and *Archeopelta arborensis* are currently considered erpetosuchids; see Ezcurra et al., 2017; Foffa et al., 2020). Additionally, in our dataset (a derivation of the same one used by Bennett) *Scleromochlus taylori*, which lacks osteoderms, lacks the only two unambiguous (osteoderm-related) synapomorphies of Doswelliidae (Sues et al., 2013). *Scleromochlus* also lacks other typical doswelliid features, such as a wide and low body (due to the lateral orientation of the ribs) and pterygoid teeth. True similarities are limited to the proportionally large head (although this is due to the long snout in *Doswelliia*) and the forelimb being shorter than the hindlimbs, both of which are features present in multiple archosaur groups. In our analyses Doswelliidae is one of the closest outgroups to Archosauria (Ezcurra, Jones, et al., 2020; Sues et al., 2013), and forcing *Scleromochlus* in this group requires 22 additional steps (5059) compared with the MPTs from our primary analysis.

5.1.3 | *Scleromochlus taylori* in Pseudosuchia

In our analysis, Pseudosuchia is supported by 15 unambiguous character states (see Data S2). Of these, *Scleromochlus* has only one, a mediolaterally expanded distal end of the tibia, but it does not share the states for six other characters that could be scored (i.e., sculpturing on the skull; spine tables present on dorsal and cervical vertebrae; fibular condyle of the femur projecting beyond the tibial condyle; distally tapering medial condyle of the femur; prominent tubercle for the attachment of the iliofibularis muscle present on the fibula; pedal ungual with a sharp dorsal keel), and it cannot be scored for the remaining eight characters. Among the latter there are several historical characters, such as those pertaining to the ankle, that cannot be verified because of uncertainty in interpreting the anatomy of this region in *Scleromochlus* (see Foffa et al., 2022). Importantly, Foffa et al. (2022) demonstrated that even when scored with a "crurotarsal"-like ankle, *Scleromochlus* falls within Pterosauromorpha. Additionally, it is noteworthy that a "crurotarsal"-like ankle morphology is not conclusive of pseudosuchian affinities, as it has been shown to be present at the base of Avemetatarsalia (Nesbitt et al., 2017). Overall, forcing *Scleromochlus* in Pseudosuchia requires 49 additional steps (5086) compared with the MPTs from our primary analysis.

When considered to lie within Pseudosuchia, *Scleromochlus* was often (and usually uncritically) considered closely related to Ornithosuchidae (Broom, 1913; Watson, 1917), based on superficial and unspecified cranial similarities. We do not find any noteworthy similarities between ornithosuchids and *Scleromochlus taylori*.

Currently, *Scleromochlus* has a single feature that is otherwise a synapomorphy of Ornithosuchidae: the presence of a supinator groove on the distal end of the humerus. It does not share nine other character states that define this clade, and it cannot be scored for the remaining 20. Overall, forcing *Scleromochlus* in Ornithosuchidae requires 33 additional steps (5072) compared with the MPTs from our primary analysis.

5.1.4 | *Scleromochlus taylori* in Avemetatarsalia: Aphanosauria, Dinosauromorpha, Silesauridae

The body plan of *Scleromochlus* shares some characteristics with aphanosaurs, basal dinosauromorphs and silesaurids (Foffa et al., 2022). Although we consider these similarities to be retained plesiomorphies, here we take a closer look at the diagnostic traits of Silesauridae, Aphanosauria, and Dinosauromorpha and discuss the historical referrals of *Scleromochlus* to these groups.

In our analysis, four character states justify the inclusion of *Scleromochlus* in Avemetatarsalia (i.e., a proportionally narrow scapula; a small acetabulum compared with the length of the femur; presence of a well-developed preacetabular process; and a supracetabular crest that is confluent with the preacetabular process). *Scleromochlus* does not possess a convex dorsal margin of the iliac blade and cannot be scored for the remaining seven unambiguous autapomorphies of Avemetatarsalia.

Scleromochlus cannot be scored for only one unambiguous synapomorphy of Aphanosauria in our analysis (i.e., anteriorly curved anterior margin of the neural spines on anterior and middle postaxial cervical vertebrae). Furthermore, it lacks elongated cervical vertebrae, a large deltopectoral crest, and a wide distal end of the humerus, all of which are considered as diagnostic characters of aphanosaurs (Nesbitt et al., 2017).

In our analyses Sileseauridae is supported by five character states (see Data S1), none of which can be verified in *Scleromochlus*.

Dinosauromorpha is supported by 13 unambiguous synapomorphies in our analysis. *Scleromochlus* can be unambiguously scored for seven of them but shares none of their states. Historically, Sereno (1991) argued that five synapomorphies could unite *Scleromochlus* and Dinosauromorpha, but these were criticized by Benton (1999). We largely agree with Benton's rebuttal of these features.

Overall, forcing *Scleromochlus* to be an "indeterminate" basal member (non-aphanosaurian, non-dinosauromorph, non-silesaruid, non-pterosaur avemetatarsalian) of Avemetatarsalia (see Nesbitt et al., 2017) requires between 133 additional steps (total

of 5170) compared with the MPTs from our primary analysis (see Section 4; Table 2).

5.1.5 | *Scleromochlus taylori* in Pterosauromorpha

The effects of the μCT scan data in supporting the position of *Scleromochlus* in Pterosauromorpha have already been discussed (Foffa et al., 2022), so we only summaries them here. The inclusion of *Scleromochlus* in Pterosauromorpha is based on one of three unambiguous features (i.e., concave anterior margin of the maxilla). Note that the inclusion of *Maehary bonapartei* caused changes to the synapomorphies of Pterosauromorpha compared with Ezcurra, Jones, et al. (2020) and Foffa et al. (2022), with many of these features now diagnostic of Lagerpetidae + Pterosauria (i.e., all pterosauromorphs more deeply nested than *Maehary*). New data from the skull, femur, and pelvis, further strengthen the placement of *Scleromochlu*s in Pterosauromorpha (see Description, above; Foffa et al., 2022). Through the years, several features have been proposed to unite *Scleromochlus taylori* and pterosaurs. Based on our results, some of these could be now considered diagnostic of less inclusive groups instead (e.g., the length of the skull versus presacral column length; Padian, 1984; Gauthier, 1984, 1986; Sereno, 1991; N.B., no complete lagerpetid skull or vertebral series is available to confirm this hypothesis); some are secondarily lost in Lagerpetidae (e.g., metatarsal I and III subequal in length—based on *Lagerpeton chanarensis*; radius and humerus subequal in length; Sereno, 1991); and others are unverifiable in a sufficiently large sample of taxa. Similarly, a handful of historical putative synapomorphies of *Scleromochlus taylori* + Pterosauria have subsequently been disproved (e.g., the absence of a fourth trochanter; Sereno, 1991), abandoned (e.g., trapezoidal pelvis; Gauthier, 1984), or demonstrated to be more widespread than previously appreciated (e.g., the metatarsal/tibia/femur ratios; Gauthier, 1986) (see Nesbitt et al., 2017).

Within Pterosauromorpha, our analysis recovers *Scleromochlus taylori* as a lagerpetid, sharing with this group four out of its five unambiguous synapomorphies. This placement is more parsimonious than a position at the base of Pterosauromorpha (Ezcurra, Jones, et al., 2020; Kammerer et al., 2020), or as the sister taxon to Pterosauria (Gauthier, 1984, 1986; Padian, 1984; Sereno, 1991). The close affinity of *Scleromochlus* with Lagerpetidae is not a new finding, but it is much more strongly supported here than in any previous study

(Figures 13 and 14). Similarities between *Scleromochlus* and *Lagerpeton* were noted by Romer (1971a), who included the latter in Scleromochlidae (within Pseudosuchia), but he offered no explanation in support of this hypothesis. More recently, Nesbitt et al. (2017) recovered *Scleromochlus taylori* in a large polytomy with aphanosaurs, *Spondylosoma*, pterosaurs, lagerpetids, and dinosauriforms, using a dataset derived from Nesbitt (2011). *Scleromochlus* was there found within Lagerpetidae, which was composed of (*L. chanarensis*, *D. romeri*, and *D. gregorii*) in some of the MPTs. The same study also found *Scleromochlus* in Dinosauromorpha (*sensu* Sereno et al., 2005) and in a polytomy with Lagerpetidae and Dinosauriformes, using a dataset derived from Ezcurra's (2016) matrix. The uncertain position of *Scleromochlus taylori* was explained by the missing information for character states from key areas of the skeleton (i.e., the femur, ankle, and pelvis) that are known to optimize at the base of Avemetatarsalia (Nesbitt et al., 2017). Even in the absence of μCT scan data, the hypothesis that *Scleromochlus taylori* is closely related to Lagerpetidae gained weight with the discovery and inclusion of additional lagerpetids (PVSJ 883, *Ixalerpeton polesinensis*, *Kongonaphon kely*) into these datasets. Kammerer et al. (2020) recovered *Scleromochlus taylori*, Lagerpetidae and Pterosauria in a polytomy with Dinosauriformes (using a dataset derived from Nesbitt, 2011), while Ezcurra, Jones, et al. (2020) recovered *Scleromochlus* outside Pterosauria + Lagerpetidae. In the latter work, *Scleromochlus taylori* still acted as a wild card, giving support to Nesbitt et al.'s (2017) observation on the importance of missing key information. We have now largely clarified this once-missing information using μCT data.

5.2 | *The affinities of* Maehary *and* Faxinalipterus

Our new data cement the inclusion of *Scleromochlus taylori* in Lagerpetidae, and the relationships within Pterosauromorpha, which are well supported in both of our analyses. Conversely, the inclusion of *Maehary bonapartei* and *Faxinalipterus minimus* introduces uncertainties into the phylogenies and inconsistencies between the maximum parsimony and Bayesian inference analyses. The lack of clear, unambiguous synapomorphies within subclades of archosaurs (i.e., hook-like femoral head of Lagerpetidae; see discussion in Kellner et al., 2022) and the incompleteness of many lagerpetids are likely responsible for this mismatch and for the increases in the numbers of MPTs recovered and their tree lengths between this analysis and that of Foffa et al. (2022).

Faxinalipterus is ~98% incomplete and cannot be scored for any of the optimized synapomorphies of lagerpetids, lagerpetids + pterosaurs, or pterosauromorphs. Kellner et al. (2022) understood the difficulty of including *Faxinalipterus* in Lagerpetidae, noticing that the combination of two character states that supported this phylogenetic position (i.e., the presence of an enlarged tuber and the absence of cranial tuber on proximal femoral head) is composed of characters that might also be treated as missing entries. In our analysis, these features are not diagnostic, so the inclusion of *Faxinalipterus* in Lagerpetidae is due exclusively to the optimization of character states that are widespread and convergent among clades within Archosauromorpha (Kellner et al., 2022). This is especially problematic in a group like Lagerpetidae where many taxa are missing >95% of their character scores. In our opinion, incompleteness, and the lack of key synapomorphic features, are thus responsible for the inconsistent positions of *Faxinalipterus* in the maximum parsimony and Bayesian inference trees. The most notable consequence of this concerns the monophyly of *Dromomeron* within Lagerpetidae (see also Müller et al., 2023).

In the maximum parsimony analysis, *Faxinalipterus* is found as the sister taxon to *Dromomeron gregorii*, in a polytomy with other lagerpetids and (*D. romeri* + *D. gigas*) (Figure 13). This is not the case in the Bayesian inference analysis, which maintains a monophyletic *Dromomeron* lineage, with *Faxinalipterus* and PVSJ 883 at its root (Figure 14). *Faxinalipterus* does not possess a clear synapomorphy of *Dromomeron* so, once again, its position is the result of the overlapping combination of common character states—many of which cannot be verified in these taxa. Indeed, in our opinion, the strongest arguments for the inclusion of *Faxinalipterus* in Lagerpetidae lie in features it shares with *Scleromochlus* (e.g., a slender humerus with a short and weakly developed triangular deltopectoral crest). Unfortunately, these features are not diagnostic of Lagerpetidae or Pterosauromorpha. In this respect, the phylogenetic position of *Faxinalipterus* is effectively determined by a handful of plesiomorphies in a few taxa, and its inclusion in Lagerpetidae and Pterosauromorpha should be treated with caution, as suggested by Kellner et al. (2022). Concerning the monophyly of *Dromomeron*, we do not think that the result from the maximum parsimony analysis is sufficient to overrule the more robust uncoded synapomorphies that unite the species of this genus (Griffin et al., 2019; Irmis et al., 2007; Marsh, 2018; Martínez et al., 2016; Müller et al., 2018; Nesbitt et al., 2009). Note that *Faxinalipterus* was subjected to rescoring in a recent study that

has recovered this taxon as the earliest diverging member of Pterosauromorpha (Müller et al., 2023).

Although more complete, similar issues affect the phylogenetic position of *Maehary bonapartei* and its inclusion in Pterosauromorpha. Currently, *Maehary bonapartei* possesses two previously identified synapomorphies of Pterosauromorpha (i.e., concave anterior margin of the maxilla; lack of tooth serrations) and a novel one that cannot be verified in any lagerpetid (i.e., thin premaxillary prenarial process). However, *Maehary bonapartei* does not possess any of the identified autapomorphies of Lagerpetidae + Pterosauria, which were, until recently, diagnostic of Pterosauromorpha as a whole. Furthermore, it cannot be scored for any of the synapomorphies of Lagerpetidae. Similarly, the incompleteness of most lagerpetid crania and *Maehary bonapartei* is a fundamental issue affecting resolution in this area of the tree because it makes it difficult to compare their anatomy with those of other pterosauromorphs (including *Scleromochlus*). The inconsistency between the results of the Bayesian inference and maximum parsimony topologies, and the impossibility of verifying the presence/absence of key features (due to the fragmentary preservation of all of these taxa), should raise concerns regarding the inclusion of *Maehary* in Pterosauromorpha. The uncertain phylogenetic affinities of *Maehary bonapartei* are highlighted further by a recent study that, after rescoring the taxon, recovered it as a gracilisuchid pseudosuchian (Müller et al., 2023).

In this scenario, the completeness of *Scleromochlus*, which is one of the most complete non-dinosaurian non-pterosaur ornithodirans, is particularly important because it provides much-needed reference data for comparisons. Our present inability to compare important features across all members of Pterosauromorpha is problematic because it reduces the diagnostic power of certain characters and adds uncertainty to the optimization of others. Similar issues likely affected the internal relationships of Pterosauria in Foffa et al. (2022), which were less resolved than in Ezcurra, Jones, et al. (2020). The inclusion of two additional Triassic pterosaurs *Yelaphomte* and *Pachagnathus* in this work rectified that issue (at least in the maximum parsimony analysis). Unfortunately, increasing resolution within Lagerpetidae and at the base of Pterosauromorpha will be more complex because of the incompleteness of the taxa in this part of the tree. Accordingly, only the addition of more complete specimens of *Scleromochlus*, lagerpetids and *Maehary*, ideally with overlapping anatomy, will help bridge the morphological gaps between pterosauromorph lineages.

5.3 | Nomenclature

Finally, the main nomenclatural consequence of this work concerns the validity of the family Scleromochlidae Huene, 1914 and whether this name should be used within Pterosauromorpha. The inclusion of *Scleromochlus taylori* in Lagerpetidae raises the nomenclatural problem that Scleromochlidae Huene, 1914 would have priority over Lagerpetidae Arcucci, 1986 (*sensu* Ezcurra, Jones, et al., 2020). However, in the interest of nomenclatural stability, and because of the unstable relationships at the base of Pterosauromorpha, we refrain from advocating this solution at present. For analogous reasons, we do not propose to reinstate the superfamily Scleromochloidea, Young, 1964 (modified from the original Scleromochliloidea (sic) by von Huene, 1914).

Instead, if new taxa are discovered that are more closely related to *Scleromochlus taylori* than to any other archosaur, we propose that Scleromochlidae Huene, 1914 could be used to define a less inclusive clade composed of forms more related to *Scleromochlus taylori* than to other lagerpetids, with the following formulation: the most inclusive clade containing *Scleromochlus taylori*, Woodward, 1907 but not *Lagerpeton chanarensis* Romer 1971, *Pterodactylus antiquus* Sommerring, 1812, *Passer domesticus* Linnaeus, 1758, or *Crocodylus niloticus* Laurenti, 1768.

6 | CONCLUSIONS

We used μCT scanning techniques to study the enigmatic Late Triassic reptile *Scleromochlus taylori*. Digital reconstructions of all the available specimens revealed numerous details and substantial parts of their skeletons that were inaccessible to previous studies, which were based primarily on molds and casts. Our study demonstrates unequivocally that data from historical casts have failed to capture the full information contained within the preserved specimens and that they can be misleading. Furthermore, taphonomic deformation was not considered sufficiently in previous studies when attempting to interpret the anatomy of *Scleromochlus*. The new and revised data presented in the current study clarify numerous aspects of the osteology of this taxon and reveal new details from all areas of the skeleton, such as the skull, trunk, tail, forelimb, and pes. We found no evidence in support of a skull that was wider than tall; the ribs of *Scleromochlus* are longer than recorded in the cast and the trunk of this animal was deeper than previously thought; the tail is long, composed of at least 50 vertebrae; and a complete foot shows that the toes increased in length from I to IV, similar to the condition in

Lagerpeton. Our revised and novel anatomical interpretations were scored into maximum parsimony and Bayesian inference analyses to revise the phylogenetic relationships of *Scleromochlus* and to test the robustness of past phylogenetic hypotheses. All our new analyses provide robust support for placing *Scleromochlus* within Avemetatarsalia, Ornithodira, and Pterosauromorpha. *Scleromochlus* is consistently found as the earliest-branching member of Lagerpetidae. Forcing *Scleromochlus* into any other position within Archosauromorpha outside of Lagerpetidae requires an increasingly high number of additional steps with respect to the original MPTs. We discuss the controversial placement of *Maehary bonapartei* and the uncertain position of *Faxinalipterus minimus* as the result of specimen incompleteness, which makes it impossible to verify the presence/absence of key diagnostic features in these taxa or to assess the genuine distributions of these character states among early avemetatarsalian lineages. In the absence of key autapomorphies, their inclusion within Pterosauromorpha should be regarded as tentative, as previously indicated by Kellner et al. (2022). We hope that our new digital data, descriptions, and illustrations set a new, more reliable, and objective benchmark for future work on *Scleromochlus* and other closely related taxa.

ORCID

Davide Foffa https://orcid.org/0000-0001-9269-6719
Sterling J. Nesbitt https://orcid.org/0000-0002-7017-1652
Richard J. Butler https://orcid.org/0000-0003-2136-7541
Stephen L. Brusatte https://orcid.org/0000-0001-7525-7319
Stig Walsh https://orcid.org/0000-0002-7002-1005
Nicholas C. Fraser https://orcid.org/0000-0003-4408-4640
Paul M. Barrett https://orcid.org/0000-0003-0412-3000

REFERENCES

Angolin, F. A., & Ezcurra, M. D. (2019). The validity of *Lagosuchus talampayensis* Romer, 1971 (Archosauria, Dinosauriformes), from the Late Triassic of Argentina. *Breviora*, *565*(1), 1–21.

Arcucci, A. (1986). Nuevos materiales y reinterpretacion de *Lagerpeton chanarensis* Romer (Thecodontia, Lagerpetonidae nov.) del Triasico Medio de La Rioja, Argentina. *Ameghiniana*, *23*(3-4), 233–242.

Bennett, S. C. (1996). The phylogenetic position of the Pterosauria within the Archosauromorpha. *Zoological Journal of the Linnean Society*, *118*(3), 261–308. https://doi.org/10.1111/j.1096-3642.1996.tb01267.x

Bennett, S. C. (2013). The phylogenetic position of the Pterosauria within the Archosauromorpha re-examined. *Historical Biology*, *25*(5-6), 545–563. https://doi.org/10.1080/08912963.2012.725727

Bennett, S. C. (2020). Reassessment of the Triassic archosauriform *Scleromochlus taylori*: neither runner nor biped, but hopper. *PeerJ*, *8*, e8418. https://doi.org/10.7717/peerj.8418

Benton, M. J. (1983). The Triassic reptile *Hyperodapedon* from Elgin: functional morphology and relationships. *Philosophical Transactions of the Royal Society of London. Series B: Biological Sciences*, *302*, 605–718. https://doi.org/10.1098/rstb.1983.0079

Benton, M. J. (1999). *Scleromochlus taylori* and the origin of dinosaurs and pterosaurs. *Philosophical Transactions of the Royal Society of London. Series B: Biological Sciences*, *354*(1388), 1423–1446. https://doi.org/10.1098/rstb.1999.0489

Benton, M. J., Donoghue, P. C. J., Asher, R. J., Friedman, M., Near, T. J., & Vinther, J. (2015). Constraints on the timescale of animal evolutionary history. *Palaeontologia Electronica*, *18*, 1–106.

Benton, M. J., & Walker, A. D. (1985). Palaeoecology, taphonomy, and dating of Permo-Triassic reptiles from Elgin, north-east Scotland. *Palaeontology*, *28*, 207–234.

Benton, M. J., & Walker, A. D. (2002). *Erpetosuchus*, a crocodile-like basal archosaur from the Late Triassic of Elgin, Scotland. *Zoological Journal of the Linnean Society*, *136*, 25–47.

Benton, M. J., & Walker, A. D. (2011). *Saltopus*, a dinosauriform from the Upper Triassic of Scotland. *Earth and Environmental Science Transactions of the Royal Society of Edinburgh*, *101*(3-4), 285–299. https://doi.org/10.1017/S1755691011020081

Broom, R. (1913). On the South-African pseudosuchian *Euparkeria* and allied genera. *Proceedings of the Zoological Society of London*, *1913*, 619–633.

Brusatte, S. L., Niedźwiedzki, G., & Butler, R. J. (2011). Footprints pull origin and diversification of dinosaur stem lineage deep into Early Triassic. *Proceedings of the Royal Society B: Biological Sciences*, *278*, 1107–1113. https://doi.org/10.1098/rspb.2010.1746

Butler, R. J., Sennikov, A. G., Dunne, E. M., Ezcurra, M. D., Hedrick, B. P., Maidment, S. C. R., Meade, L. E., Raven, T. J., & Gower, D. J. (2019). Cranial anatomy and taxonomy of the erythrosuchid archosauriform 'Vjushkovia triplicostata' Huene, 1960, from the Early Triassic of European Russia. *Royal Society Open Science*, *6*, 191289.

Cabreira, S. F., Kellner, A. W. A., Dias-da-Silva, S., Roberto da Silva, L., Bronzati, M., Marsola, J. C. A., Müller, R. T., Bittencourt, J. S., Batista, B. J., Raugust, T., Carrilho, R., Brodt, A., & Langer, M. C. (2016). A unique late triassic dinosauromorph assemblage reveals dinosaur ancestral anatomy and diet. *Current Biology*, *26*, 3090–3095.

Charig, A. J. (1967). Archosauria. In W. B. Harland (Ed.), *The fossil record: A symposium with documentation* (Vol. 2, pp. 703–718). Geological Society of London Special Publication.

Colbert, E. H. (1989). The triassic dinosaur Coelophysis. *Museum of Northern Arizona Bulletin*, *57*, 160.

Dalla Vecchia, F. M. (2013). Triassic pterosaurs. In S. J. Nesbitt, J. B. Desojo, & R. B. Irmis (Eds.), *Anatomy, phylogeny and palaeobiology of early archosaurs and their kin* (pp. 119–155). Geological Society London.

Dalla Vecchia, F. M. (2014). *Gli pterosauri triassici (Edizioni del Museo Friulano di Storia Naturale, 2014)*. Museo Friulano di Storia Naturale.

Dalla Vecchia, F. M. (2019). *Seazzadactylus venieri* gen. et sp. nov., a new pterosaur (Diapsida: Pterosauria) from the Upper Triassic (Norian) of northeastern Italy. *PeerJ*, *7*, e7363.

Dalla Vecchia, F. M. (2021). A revision of the anatomy of the Triassic pterosaur *Austriadraco dallavecchiai* Kellner, 2015 and of its diagnosis. *Research in Paleontology and Stratigraphy*, *127*(2), 427–452.

David, J., Gower, D. J., & Sennikov, A. G. (1997). *Sarmatosuchus* and the early history of the Archosauria. *Journal of Vertebrate Paleontology*, *17*(1), 60–73. https://doi.org/10.1080/02724634.1997.10010954

Davies, T. G., Rahman, I. A., Lautenschlager, S., Cunningham, J. A., Asher, R. J., Barrett, P. M., Bates, K. T., Bengtson, S., Benson, R. B. J., Boyer, D. M., Braga, J., Bright, J. A., Claessens, L. P. A. M., Cox, P. G., Dong, X.-P., Evans, A. R., Falkingham, P. L., Friedman, M., Garwood, R. J., … Donoghue, P. C. J. (2017). Open data and digital morphology. *Proceedings of the Royal Society B: Biological Sciences*, *284*, 20170194. https://doi.org/10.1098/rspb.2017.0194

Dzik, J. (2003). A beaked herbivorous archosaur with dinosaur affinities from the early Late Triassic of Poland. *Journal of Vertebrate Paleontology*, *23*, 556–574.

Ezcurra, M. D. (2016). The phylogenetic relationships of basal archosauromorphs, with an emphasis on the systematics of proterosuchian archosauriforms. *PeerJ*, *4*, e1778. https://doi.org/10.7717/peerj.1778

Ezcurra, M. D., & Butler, R. J. (2018). The rise of the ruling reptiles and ecosystem recovery from the Permo-Triassic mass extinction. *Proceedings of the Royal Society B: Biological Sciences*, *285*, 20180361. https://doi.org/10.1098/rspb.2018.0361

Ezcurra, M. D., Butler, R. J., & Gower, D. J. (2013). 'Proterosuchia': The origin and early history of Archosauriformes. In S. J. Nesbitt, J. B. Desojo, & R. B. Irmis (Eds.), *Anatomy, phylogeny and palaeobiology of early archosaurs and their kin* (pp. 9–33). Geological Society London.

Ezcurra, M. D., Fiorelli, L. E., Martinelli, A. G., Rocher, S., von Baczko, M. B., Ezpeleta, M., Taborda, J. R., Hechenleitner, E. M., Trotteyn, M. J., & Desojo, J. B. (2017). Deep faunistic turnovers preceded the rise of dinosaurs in southwestern Pangaea. *Nature Ecology & Evolution*, *1*(10), 1477–1483. https://doi.org/10.1038/s41559-017-0305-5

Ezcurra, M. D., Jones, A. S., Gentil, A. R., & Butler, R. J. (2020). Early archosauromorphs: The crocodile and dinosaur precursors. In: Reference Module in Earth Systems and Environmental Sciences. https://www.sciencedirect.com/science/article/pii/B978012409548912439X?via%3Dihub

Ezcurra, M. D., Nesbitt, S. J., Bronzati, M., Dalla Vecchia, F. M., Agnolin, F. L., Benson, R. B. J., Brissón Egli, F., Cabreira, S. F., Evers, S. W., Gentil, A. R., Irmis, R. B., Martinelli, A. G., Novas, F. E., Roberto da Silva, L., Smith, N. D., Stocker, M. R., Turner, A. H., & Langer, M. C. (2020). Enigmatic dinosaur precursors bridge the gap to the origin of Pterosauria. *Nature*, *588*, 445–449. https://doi.org/10.1038/s41586-020-3011-4

Ezcurra, M. D., Scheyer, T. M., & Butler, R. J. (2014). The origin and early evolution of Sauria: reassessing the Permian saurian fossil record and the timing of the crocodile-lizard divergence. *PLoS One*, *9*, e89165.

Ezcurra, M. D., & Cuny, G. (2007). The coelophysoid *Lophostropheus airelensis*, gen. nov.: a review of the systematics of "*Liliensternus*" airelensis from the Triassic–Jurassic outcrops of Normandy (France). *Journal of Vertebrate Paleontology*, *27*(1), 73–86.

Fitcher, J., & Kunz, R. (2013). "Dinosauromorph" tracks from the Middle Buntsandstein (Early Triassic: Olenekian) of Wolfhagen, northern Hesse, Germany. *Comunicações Geológicas*, *100*(1), 81–88.

Foffa, D., Butler, R. J., Nesbitt, S. J., Walsh, S., Barrett, P. M., Brusatte, S. L., & Fraser, N. C. (2020). Revision of *Erpetosuchus* (Archosauria: Pseudosuchia) and new erpetosuchid material from the Late Triassic 'Elgin Reptile' fauna based on μCT scanning techniques. *Earth and Environmental Science Transactions of the Royal Society of Edinburgh*, *111*(4), 209–233.

Foffa, D., Dunne, E. M., Nesbitt, S. J., Butler, R. J., Fraser, N. C., Brusatte, S. L., Farnsworth, A., Lunt, D. J., Valdes, P. J., Walsh, S., & Barrett, P. M. (2022). *Scleromochlus* and the early evolution of Pterosauromorpha. *Nature*, *610*(7931), 313–318.

Fraser, N. C., & Benton, M. J. (1989). The Triassic reptiles *Brachyrhinodon* and *Polysphenodon* and the relationships of the sphenodontids. *Zoological Journal of the Linnean Society*, *96*, 413–445.

Gauthier, J. A. (1984). A cladistic analysis of the higher systematic categories of the Diapsida [Unpublished PhD dissertation]. University of California, Berkeley, p. 564.

Gauthier, J. A. (1986). Saurischian monophyly and the origin of birds. In K. Padian (Ed.), *The origin of birds and the evolution of flight* (Vol. 8, pp. 1–55). California Academy of Sciences.

Gauthier, J. A., Kluge, A. G., & Rowe, T. (1988). Amniote phylogeny and the importance of fossils. *Cladistics*, *4*, 105–209.

Goloboff, P. A., & Catalano, S. A. (2016). TNT version 1.5, including a full implementation of phylogenetic morphometrics. *Cladistics*, *32*, 221–238.

Goloboff, P. A., Farris, J. S., & Nixon, K. C. (2008). TNT, a free program for phylogenetic analysis. *Cladistics*, *24*, 774–786. https://doi.org/10.1111/j.1096-0031.2008.00217.x

Griffin, C. T., Bano, L. S., Turner, A. H., Smith, N. D., Irmis, R. B., & Nesbitt, S. J. (2019). Integrating gross morphology and bone histology to assess skeletal maturity in early dinosauromorphs: new insights from *Dromomeron* (Archosauria: Dinosauromorpha). *PeerJ*, *7*, e6331. https://doi.org/10.7717/peerj.6331

Hone, D. W. E., Tischlinger, H., Frey, E., & Röper, M. (2012). A new non-pterodactyloid pterosaur from the late Jurassic of Southern Germany. *PLoS One*, *7*(7), e39312. https://doi.org/10.1371/journal.pone.0039312

Hyder, E. S., Witton, M. P., & Martill, D. M. (2014). Evolution of the pterosaur pelvis. *Acta Palaeontologica Polonica*, *59*(1), 109–124.

Irmis, R. B., Nesbitt, S. J., Padian, K., Smith, N. D., Turner, A. H., Woody, D., & Downs, A. (2007). A late Triassic dinosauromorph assemblage from New Mexico and the rise of dinosaurs. *Science*, *317*(5836), 358–361. https://doi.org/10.1126/science.1143325

Jenkins, F. A., Shubin, N. H., Gatesy, S. M., & Padian, K. (2001). A diminutive pterosaur (Pterosauria: Eudimorphodontidae) from the Greenlandic Triassic. *Bulletin of the Museum of Comparative Zoology*, *156*, 151–170.

Kammerer, C. F., Nesbitt, S. J., Flynn, J. J., Ranivoharimanana, L., & Wyss, A. R. (2020). A tiny ornithodiran archosaur from the Triassic of Madagascar and the role of miniaturization in dinosaur and pterosaur ancestry. *Proceedings of the National Academy of Sciences of the United States of America*, *117*, 17932–17936.

Keeble, E., & Benton, M. J. (2020). Three-dimensional tomographic study of dermal armour from the tail of the Triassic aetosaur *Stagonolepis robertsoni*. *Scottish Journal of Geology*, *56*, 55–62. https://doi.org/10.1144/sjg2019-026

Kellner, A. W., Holgado, B., Grillo, O., Pretto, F. A., Kerber, L., Pinheiro, F. L., Soares, M. B., Schultz, C. L., Lopes, R. T., Araújo, O., & Müller, R. T. (2022). Reassessment of *Faxinalipterus minimus*, a purported Triassic pterosaur from southern Brazil with the description of a new taxon. *PeerJ*, *10*, e13276.

Kellner, A. W. A. (2015). Comments on Triassic pterosaurs with discussion about ontogeny and description of new taxa. *Anais da Academia Brasileira de Ciências*, *87*(2), 669–689. https://doi.org/10.1590/0001-3765201520150307

Kuhn, O. W. M. (1966). Die reptilien. System und stammesgeschichte [The reptiles. Systematics and phylogeny.], pp. 1–154.

Kuhn, O. W. M. (1967). *Die fossile wirbeltierklasse pterosauria* (p. 52). Oeben.

Langer, M. C., Nesbitt, S. J., Bittencourt, J. S., & Irmis, R. B. (2013). Early dinosauromorpha. In S. J. Nesbitt, J. B. Desojo, & R. B. Irmis (Eds.), *Anatomy, phylogeny and palaeobiology of early archosaurs and their kin* (pp. 156–186). Geological Society London.

Langer, M. C., Ramezani, J., & Da Rosa, Á. A. S. (2018). U-Pb age constraints on dinosaur rise from south Brazil. *Gondwana Research*, *57*, 133–140. https://doi.org/10.1016/j.gr.2018.01.005

Marsh, A. D. (2018). A new record of *Dromomeron romeri* Irmis et al., 2007 (Lagerpetidae) from the Chinle Formation of Arizona, USA. *PaleoBios*, *35*, 1–8.

Martin, L. D. (1983). The origin of birds and of avian flight. *Current Ornithology*, *1*, 105–129.

Martínez, R. N., Andres, B., Apaldetti, C., & Cerda, I. A. (2022). The dawn of the flying reptiles: first Triassic record in the southern hemisphere. *Papers in Palaeontology*, *8*(2), e1424.

Martínez, R. N., Apaldetti, C., Correa, G. A., & Abelín, D. (2016). A Norian lagerpetid dinosauromorph from the Quebrada del Barro Formation, northwestern Argentina. *Ameghiniana*, *53*(1), 1–13.

Martz, J. W., & Small, B. J. (2019). Non-dinosaurian dinosauromorphs from the Chinle Formation (Upper Triassic) of the Eagle Basin, northern Colorado: *Dromomeron romeri* (Lagerpetidae) and a new taxon, *Kwanasaurus williamparkeri* (Silesauridae). *PeerJ*, *7*, e7551. https://doi.org/10.7717/peerj.7551

McCabe, M. B., Mason, B., & Nesbitt, S. J. (2021). The first pectoral and forelimb material assigned to the lagerpetid *Lagerpeton chanarensis* (Archosauria: Dinosauromorpha) from the upper portion of the Chañares Formation, Late Triassic. *Palaeodiversity*, *14*, 121–131. https://doi.org/10.18476/pale.v14.a5

Mujal, E., Fortuny, J., Bolet, A., Oms, O., & Lòpez, J. À. (2017). An archosauromorph dominated ichnoassemblage in fluvial settings from the late Early Triassic of the Catalan Pyrenees (NE Iberian Peninsula). *PLoS One*, *12*(4), e0174693. https://doi.org/10.1371/journal.pone.0174693

Müller, R. T., Ezcurra, M. D., Garcia, M. S., Agnolín, F. L., Stocker, M. R., Novas, F. E., Soares, M. B., Kellner, A. W. A., & Nesbitt, S. J. (2023). New reptile shows dinosaurs and pterosaurs evolved among diverse precursors. *Nature*, *620*(7974), 589–594. https://doi.org/10.1038/s41586-023-06359-z

Müller, R. T., Langer, M. C., & Dias-Da-Silva, S. (2018). Ingroup relationships of Lagerpetidae (Avemetatarsalia: Dinosauromorpha): A further phylogenetic investigation on the understanding of dinosaur relatives. *Zootaxa*, *4392*(1), 149–158.

Nesbitt, S., & Hone, D. W. E. (2010). An external mandibular fenestra and other archosauriform character states in basal pterosaurs. *Palaeodiversity*, *3*, 225–233.

Nesbitt, S. J. (2011). The early evolution of archosaurs: relationships and the origin of major clades. *Bulletin of the American Museum of Natural History*, *352*, 1–292. https://doi.org/10.1206/352.1

Nesbitt, S. J., Butler, R. J., Ezcurra, M. D., Barrett, P. M., Stocker, M. R., Angielczyk, K. D., Smith, R. M. H., Sidor, C. A., Niedźwiedzki, G., Sennikov, A. G., & Charig, A. J. (2017). The earliest bird-line archosaurs and the assembly of the dinosaur body plan. *Nature*, *544*, 484–487. https://doi.org/10.1038/nature22037

Nesbitt, S. J., Irmis, R. B., Parker, W. G., Smith, N. D., Turner, A. H., & Rowe, T. (2009). Hindlimb osteology and distribution of basal dinosauromorphs from the late triassic of North America. *Journal of Vertebrate Paleontology*, *29*(2), 498–516.

Nesbitt, S. J., Langer, M. C., & Ezcurra, M. D. (2020). The Anatomy of *Asilisaurus kongwe*, a dinosauriform from the lifua member of the Manda Beds (~Middle Triassic) of Africa. *Anatomical Record*, *303*, 813–873. https://doi.org/10.1002/ar.24287

Nesbitt, S. J., & Norell, M. A. (2006). Extreme convergence in the body plans of an early suchian (Archosauria) and ornithomimid dinosaurs (Theropoda). *Proceedings of the Royal Society B: Biological Sciences*, *273*(1590), 1045–1048.

Nesbitt, S. J., Sidor, C. A., Irmis, R. B., Angielczyk, K. D., Smith, R. M. H., & Tsuji, L. A. (2010). Ecologically distinct dinosaurian sister group shows early diversification of Ornithodira. *Nature*, *464*(7285), 95–98. https://doi.org/10.1038/nature08718

Newton, E. T. (1894). Reptiles from the Elgin sandstone. Description of two new genera. *Philosophical Transactions of the Royal Society of London. Series B: Biological Sciences*, *185*, 573–607.

Niedźwiedzki, G., Brusatte, S. L., & Butler, R. J. (2013). *Prorotodactylus* and *Rotodactylys* tracks: an ichnological record of dinosauromorphs from the Early-Middle Triassic of Poland. In S. J. Nesbitt, J. B. Desojo, & R. B. Irmis (Eds.), *Anatomy, Phylogeny and Palaeobiology of Early Archosaurs and their Kin* (pp. 319–351). Geological Society London.

Padian, K. (1984). The origin of pterosaurs. In W.-E. Reif & F. Westphal (Eds.), *Third symposium on mesozoic terrestrial ecosystems, short papers* (pp. 163–168). Tübingen.

Padian, K. (2008). Were pterosaur ancestors bipedal or quadrupedal? Morphometric, functional, and phylogenetic considerations. *Zitteliana*, *B28*, 21–33.

Padian, K. (2012). The problem of dinosaur origins: integrating three approaches to the rise of Dinosauria. *Earth and Environmental Science Transactions of the Royal Society of Edinburgh*, *103*, 423–442.

Rahhut, O. W. M. (2003). The interrelationships and evolution of basal theropod dinosaurs. *Special Papers in Palaeontology*, *69*, 1–213.

Romer, A. S. (1956). Osteology of the Reptiles. *University of Chicago Press*, 1–772.

Romer, A. S. (1966). *Vertebrate paleontology* (3rd ed., pp. 1–468). The University of Chicago Press.

Romer, A. S. (1971a). The Chañares (Argentina) Triassic reptile fauna. X. Two new but incompletely known long-limbed pseudosuchians. *Breviora*, *378*, 1–10.

Romer, A. S. (1971b). The Chañares (Argentina) Triassic reptile fauna. XVI. Thecodont classification. *Breviora*, *395*, 1–24.

Ronquist, F., van der Mark, P., & Huelsenbeck, J. P. (2009). Bayesian phylogenetic analysis using MRBAYES. In P. Lemey, M. Salemi, & A.-M. Vandamme (Eds.), *The phylogenetic handbook: A practical approach to phylogenetic analysis and hypothesis testing* (pp. 210–266). Cambridge University Press.

Säilä, L. (2010). Osteology of *Leptopleuron lacertinum* Owen, a procolophonoid parareptile from the Upper Triassic of Scotland, with remarks on ontogeny, ecology and affinities. *Earth and Environmental Science Transactions of the Royal Society of Edinburgh*, *101*(1), 1–25. https://doi.org/10.1017/S1755691010009138

Sereno, P. C. (1991). Basal archosaurs: phylogenetic relationships and functional implications. *Journal of Vertebrate Paleontology*, *11*(suppl 4), 1–53. https://doi.org/10.1080/02724634.1991.10011426

Sereno, P. C., & Arcucci, A. B. (1994). Dinosaurian precursors from the Middle Triassic of Argentina: *Lagerpeton chanarensis*. *Journal of Vertebrate Paleontology*, *13*(4), 385–399. https://doi.org/10.1080/02724634.1994.10011522

Sereno, P. C., McAllister, S., & Brusatte, S. L. (2005). TaxonSearch: a relational database for suprageneric taxa and phylogenetic definitions. *PhyloInformatics*, *8*, 1–21.

Spiekman, S. N. F., Ezcurra, M. D., Butler, R. J., Fraser, N. C., & Maidment, S. C. R. (2021). Pendraig milnerae, a new small-sized coelophysoid theropod from the Late Triassic of Wales. *Royal Society Open Science*, *8*(10), 210915. https://doi.org/10.1098/rsos.210915

Sues, H.-D., Desojo, J. B., & Ezcurra, M. D. (2013). Doswelliidae: a clade of unusual armoured archosauriforms from the Middle and Late Triassic. In S. J. Nesbitt, J. B. Desojo, & R. B. Irmis (Eds.), *Anatomy, phylogeny and palaeobiology of early archosaurs and their kin* (pp. 49–58). Geological Society London.

Swinton, W. E. (1960). The origin of birds. In A. J. Marshall (Ed.), *Biology and comparative physiology of birds* (Vol. 1, pp. 1–14). Academic Press.

Swinton, W. E. (1970). *The dinosaurs* (pp. 1–331). Wiley-Interscience.

Von Baczko, M. B., & Ezcurra, M. D. (2016). Taxonomy of the archosaur *Ornithosuchus*: reassessing *Ornithosuchus woodwardi* Newton, 1894 and *Dasygnathoides longidens* (Huxley 1877). *Earth and Environmental Science Transactions of the Royal Society of Edinburgh*, *106*, 199–205.

von Huene, F. (1908). Die dinosaurier der europaiaschen triasformation mit berucksichtiging der aussereuropaischen vorkommnisse. *Geologische und paläontologische Abhandungen*, *1*, 1–419.

von Huene, F. (1913). Über die reptilführenden sandsteine bei elgin in Schottland. *Centralblatt für Mineralogie, Geologie und Paläontologie*, *1*, 617–623.

von Huene, F. (1914). Beiträge zur geschichte der archosaurier. *Geologische und paläontologische Abhandungen*, *13*, 3–53.

von Huene, F. (1922). The triassic reptilian order thecodontia. *The American Journal of Science*, *5*(4), 22–26.

von Huene, F. (1942). Lieferungen 3/4. Pseudosuchia, Saurischia, Rhynchosauridae und Schlussabschnitt [Parts 3/4. Pseudosuchia, Saurischia, Rhynchosauridae, and Conclusions]. Die Fossilen Reptilien des Südamerikanischen Gondwanalandes. Ergebnisse der Sauriergrabungen in Südbrasilien 1928/29. [The Fossil Reptiles of South American Gondwanaland. Results of the Dinosaur Expeditions in southern Brazil 1928/29]. C. H. Beck'sche Verlagsbuchhandlung, München, pp. 161–332.

Walker, A. D. (1964). Triassic reptiles from the Elgin area: *Ornithosuchus* and the origin of carnosaurs. *Philosophical Transactions of the Royal Society of London. Series B: Biological Sciences*, *248*(744), 53–134.

Walker, A. D. (1970). A revision of the Jurassic reptile *Hallopus victor* (Marsh), with remarks on the classification of crocodiles. *Philosophical Transactions of the Royal Society of London. Series B: Biological Sciences*, *257*, 323–372.

Watson, D. M. S. (1917). A sketch classification of the Pre-Jurassic tetrapod vertebrates. *Proceedings of the Zoological Society of London*, *1917*, 167–186.

Wellnhofer, P. (2003). A Late Triassic pterosaur from the Northern Calcareous Alps (Tyrol, Austria). *Geological Society, London, Special Publications*, *217*(1), 5–22.

Wild, R. (1978). Die Flugsaurier (Reptilia, Pterosauria) aus der Oberen Trias von Cene bei Bergamo. *Bollettino della Societa Paleontologica Italiana*, *17*, 176–256.

Wild, R. (1984). A new pterosaur (Reptilia, Pterosauria) from the Norian (Late Triassic) of Friuli (Northeastern Italy). *Gortania*, *5*, 45–62.

Woodward, A. S. (1907). On a new dinosaurian reptile (*Scleromochlus taylori*, gen. et sp. nov.) from the Trias of Lossiemouth, Elgin. *Quarterly Journal of the Geological Society*, *63*(144), 140. https://doi.org/10.1144/GSL.JGS.1907.063.01-04.12

Yáñez, I., Pol, D., Leardi, J. M., Alcober, O. A., & Martínez, R. N. (2021). An enigmatic new archosauriform from the Carnian–Norian, Upper Triassic, Ischigualasto Formation of northwestern Argentina. *Acta Palaeontologica Polonica*, *66*(3), 509–533.

Young, C. C. (1964). On a new pterosaurian from Sinkiang, China. *Vertebrata PalAsiatica*, *8*, 221–255.

Zanno, L. E., & Makovicky, P. J. (2011). Herbivorous ecomorphology and specialization patterns in theropod dinosaur evolution. *Proceedings of the National Academy of Sciences*, *108*(1), 232–237.

SUPPORTING INFORMATION

Additional supporting information can be found online in the Supporting Information section at the end of this article.